Basics of TES microcalorimeter/ bolometer and non-astronomy applications

Kazuhisa Mitsuda
QUP, KEK,
Advanced Technology Center, National Astronomical Observatory of Japan, NINS
and
ISAS/JAXA (professor emeritus)

(Except for the last section, today's talk is based on the research while I was at ISAS/JAXA.)

CMB B-mode NEXT workshop @KEK in Tsukuba on 28 January 2025

Tommaso asked me

- An overview talk about superconducting detectors for CMB, X-ray astronomy, DM search, and beyond.

- However, I decided to emphasize applications other than CMB, X-ray astronomy, and DM search; they have quite different requirements than X-ray astronomy, etc.

Talk plan

	Example application
• Introduction to microcalorimeters (10 min)	X-ray astronomy (Semiconductor-type) Nuclear spectroscopy (MMC)
• Basics of TES microcalorimeters (25 min)	Martial science (TES μ-calorimeter)
• Basics of TES bolometers (5 min, since all necessary items have already been presented)	
• Example application, which I am interested in now (5 min)	
• 0-th order design study of the new TES bolometers for non-astronomy application	New non-astronomy application (TES bolometer)

Introduction to microcalorimeters

Microcalorimeters

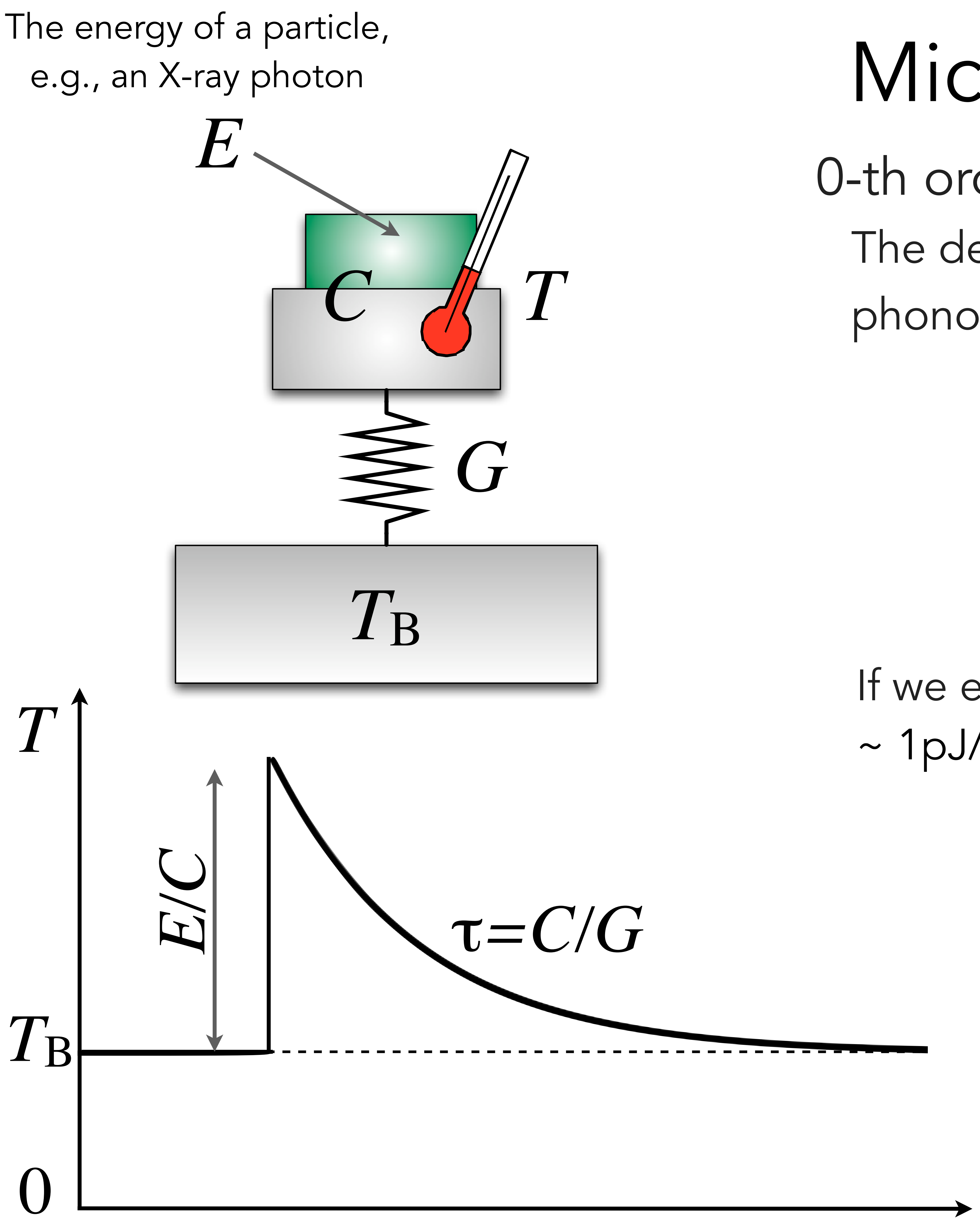

(The above plot is wrong if the thermometer is dissipating heat.)

0-th order estimation of energy resolution:

The detector thermal energy ($U = CT$) fluctuates, since the number of phonons fluctuates. With the average phonons energy $\epsilon = k_B T$,

$$\sigma_E = \sqrt{\frac{U}{\epsilon}}\epsilon = \sqrt{\frac{CT}{k_B T}}k_B T = \sqrt{k_B T^2 C}$$

This factor will appear in energy-resolution equations.

If we estimate using this factor, for a 100μm-square, 5μm-thick metal absorber C ~ 1pJ/K@100mK, we obtain,

FWHM resolution: $\Delta E = 2.35\sigma_E \sim 5$ eV

This is about 30 times better compared to semiconductor detectors for 1-10 keV X-rays.

Real energy resolution depends on the type of thermometer we use.

What is the energy resolution ?

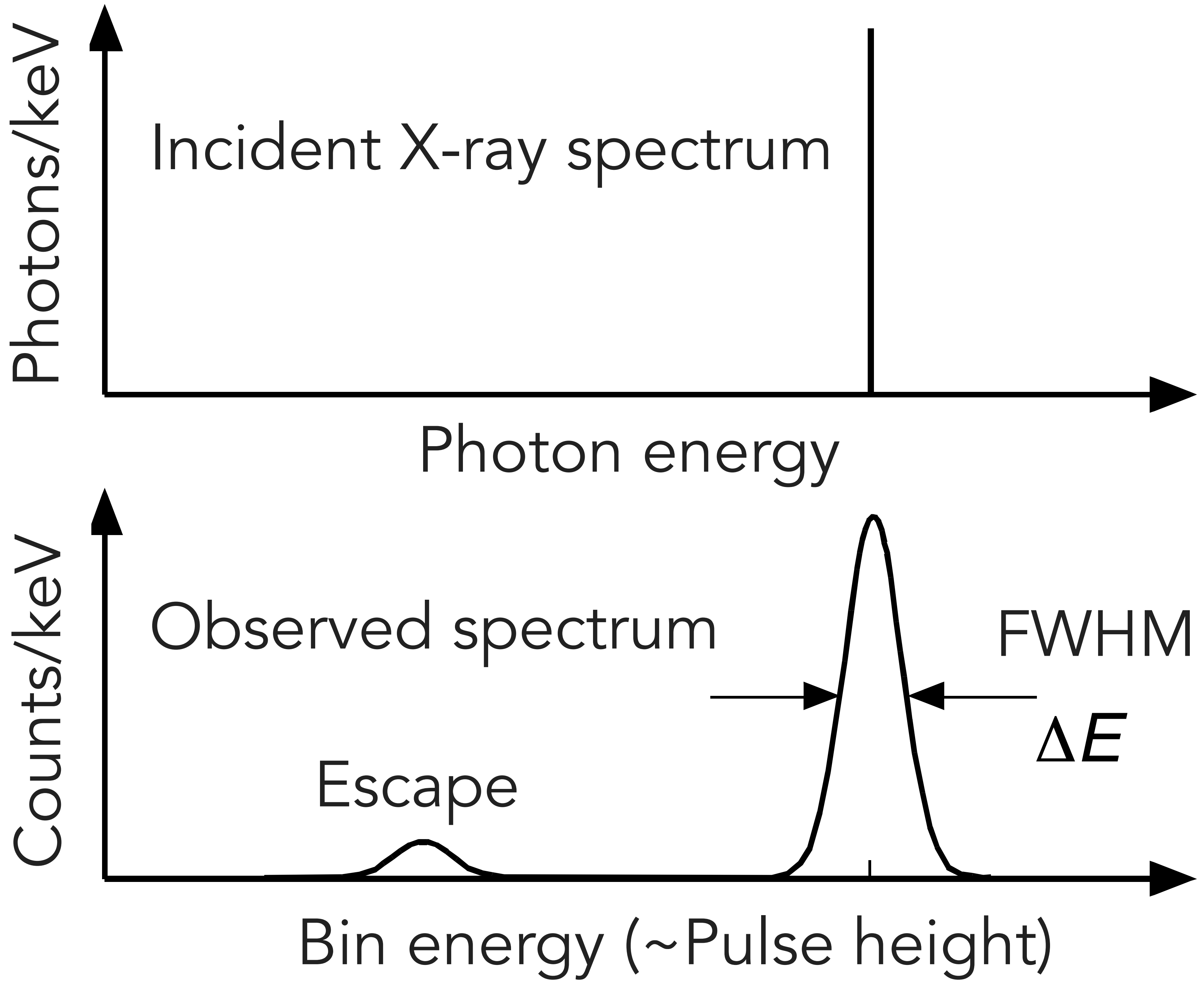

STEM EDS

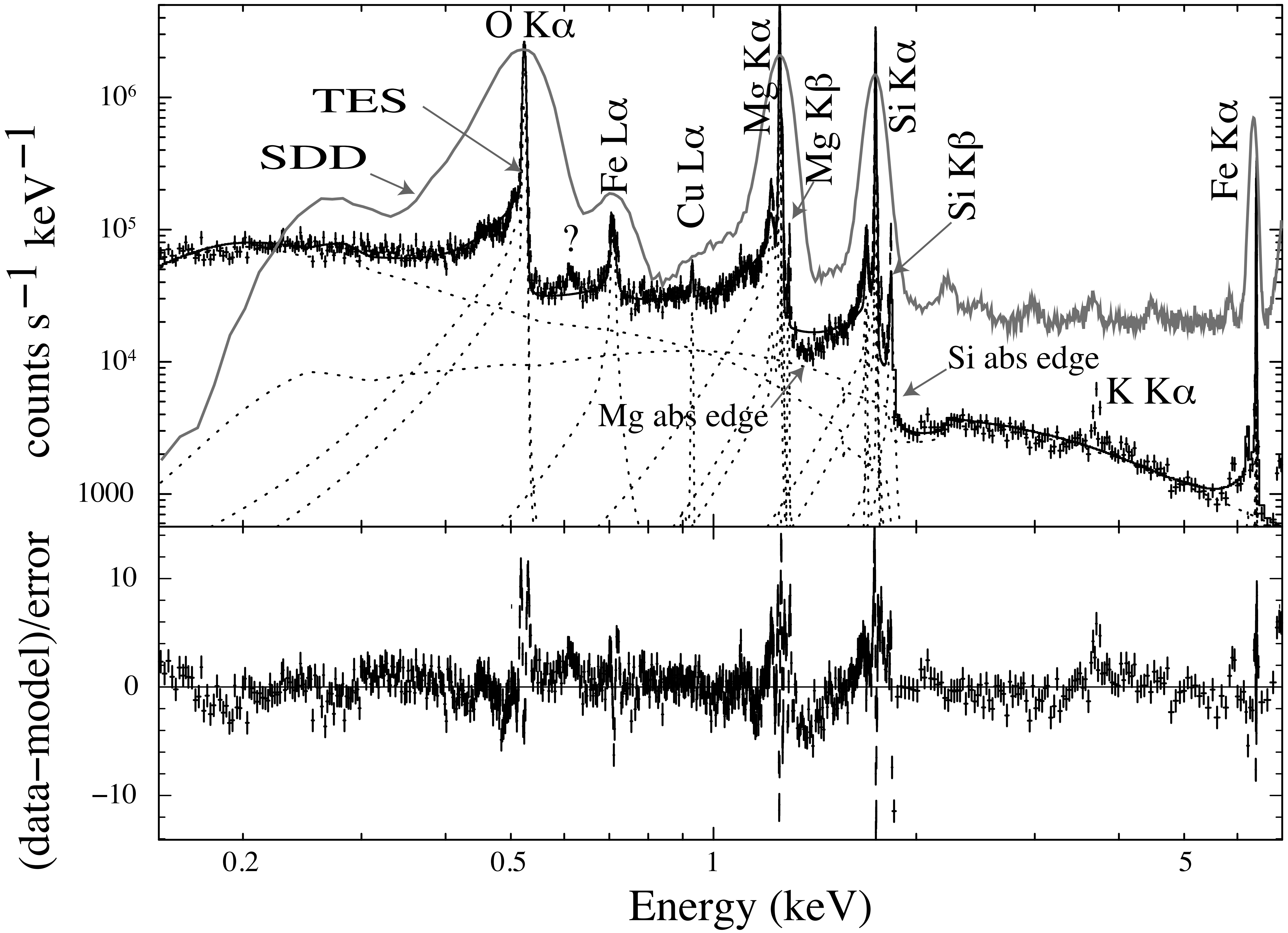

Hayashi (2019)
Hayashi, .. KM + (2018)

Thermometer types

Established as X- and γ-ray detectors (upper three rows)

Type	Dissipative?	Remarks
Semiconductor type	Yes	First practical thermometers both for microcalorimeters and bolometers. *Slow time response*. *Signal multiplexing is NOT possible* because of high impedance.
TES type	Yes	**Faster response** than semiconductor type. **Signal multiplexing** is possible because of low impedance. *Larger non-linearity* in the response than semiconductor type.
Metalic-Magnetic type	No	*Slow time response*. **Signal multiplexing** is possible with SQUID readout. **Good linearity** in the response compared to the above two types.
Microwave Kinetic-Inductance type	No	So-called thermal KIDs. Signal multiplex is possible. The energy resolution as good as those of semiconductor- and TES-types have NOT been obtained.
Dielectric Type	No	Low TRL (Technology Readiness Level): only confirmed to work as a microcalorimeter and a bolometer (Yoshimoto, KM+ 2019, Yamasaki, KM+ 2015). TLS (Two-level system) noise will limit the ultimate performance. Signal multiplex is possible.

FYI: Naming conventions recommended by IEC for superconductor devices

IEC = **I**nternational **E**lectrotechnical **C**ommission

IEC 61788-22-1

IEC 61788-22-1:2017

Superconductivity - Part 22-1: Superconducting electronic devices - Generic specification for sensors and detectors

IEC 61788-22-1:2017 describes general items concerning the specifications for superconducting sensors and detectors, which are the basis for specifications given in other parts of IEC 61788 for various types of sensors and detectors. The sensors and detectors described are basically made of superconducting materials and depend on superconducting phenomena or related phenomena. The objects to be measured (measurands) include magnetic fields, electromagnetic waves, photons of various energies, electrons, ions, a-particles, and others.

Show less

BASE PUBLICATION

Language	English
Format	Electronic
User	1

CHF 190.- Add to cart

Dr. M. Ohkubo at AIST was the chair of the committee that proposed this document.

I was a committee member.

Semiconductor-type calorimeter

$$\Delta E = \xi \sqrt{k_B T^2 C}$$

$$\alpha = \frac{d \log R}{d \log T} = -3 \text{ to } -10$$

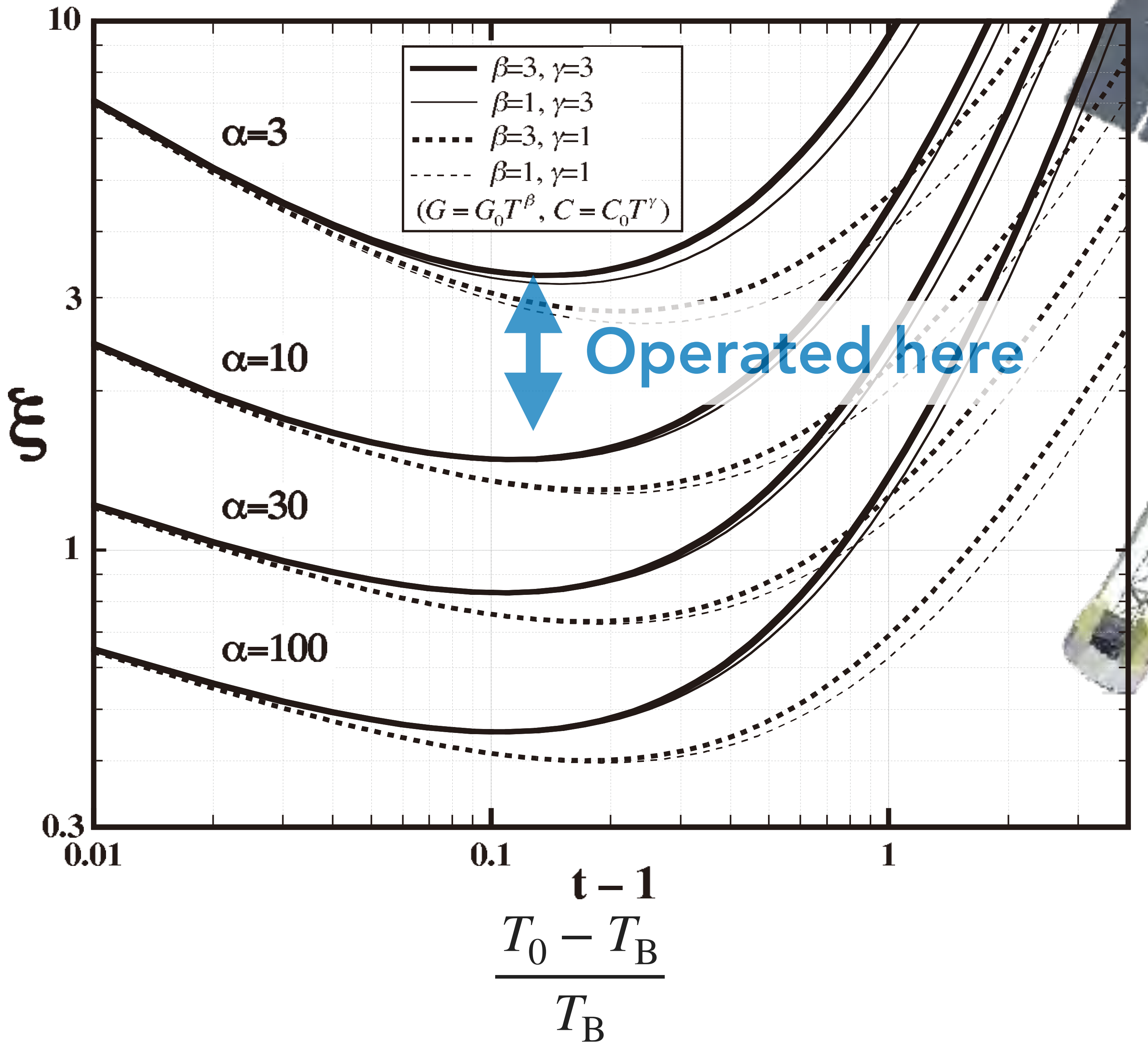

Moseley, Mather, & McCammon (1984)
McCammon (2005)

ASTRO-H

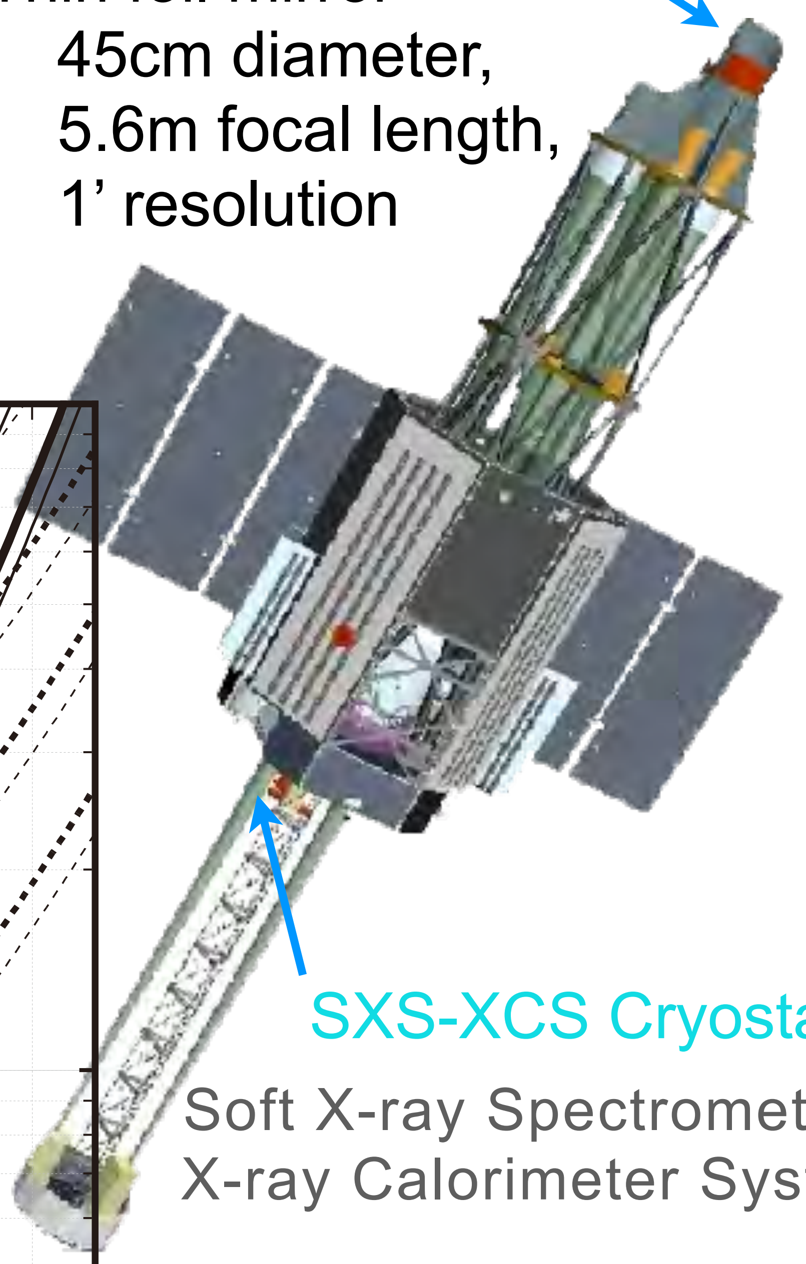

Thin foil mirror
45cm diameter,
5.6m focal length,
1' resolution

Soft X-ray Spectrometer - X-ray Calorimeter System

6x6 μ-calorimeter array
≤ 7 eV resolution
2.9x2.9' FOV

ASTRO-H SXS & XRISM Resolve

SXS detector

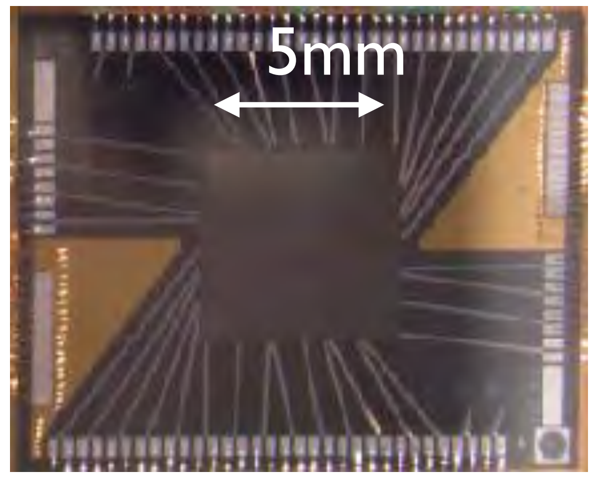

6x6 format, 36 pixel **semiconductor-thermometer** microcalorimeter array made by NASA/GSFC

Perseus cluster

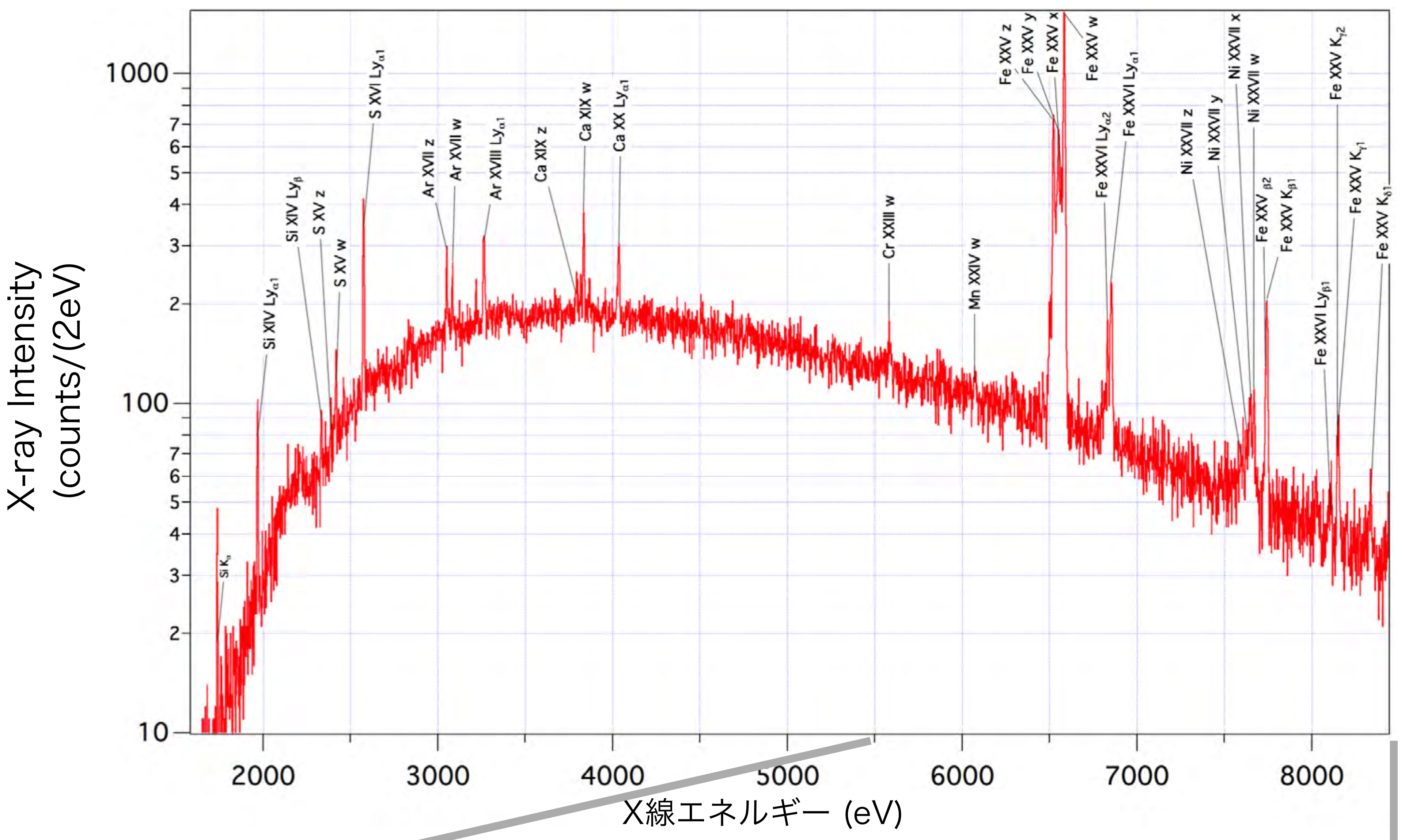

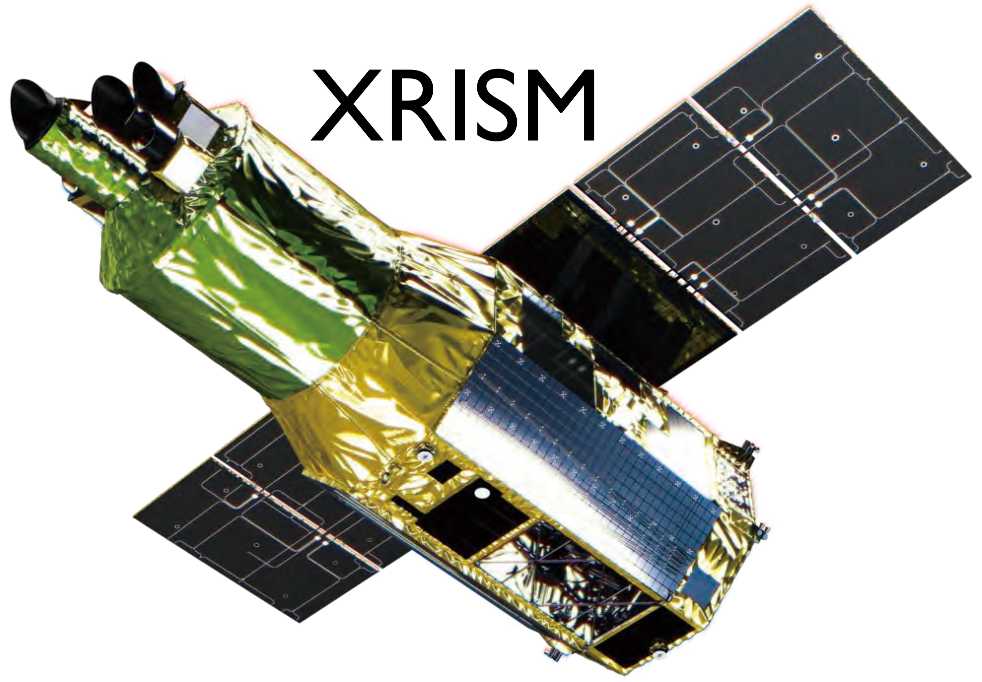

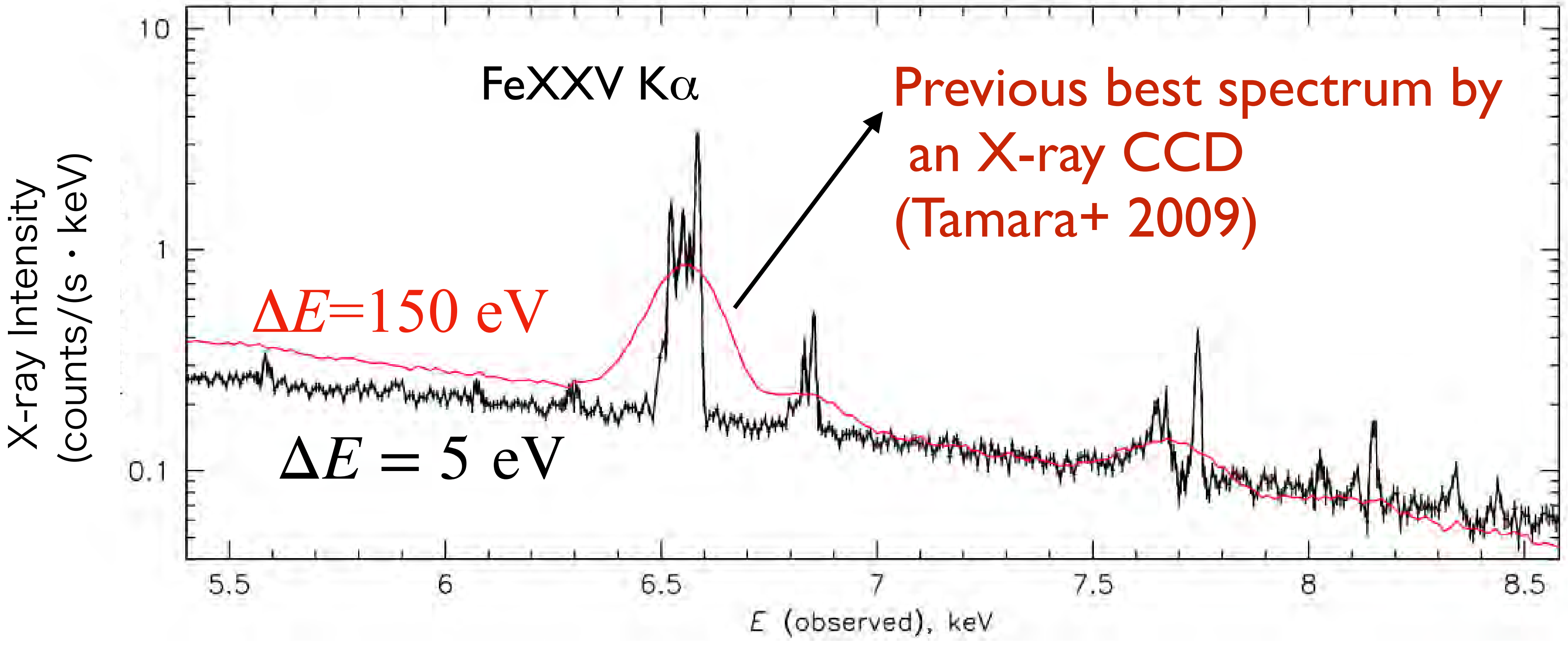

Hitomi collaborations incl. KM (2016)

Metalic-Magnetic-type μ-Calorimeter (MMC)

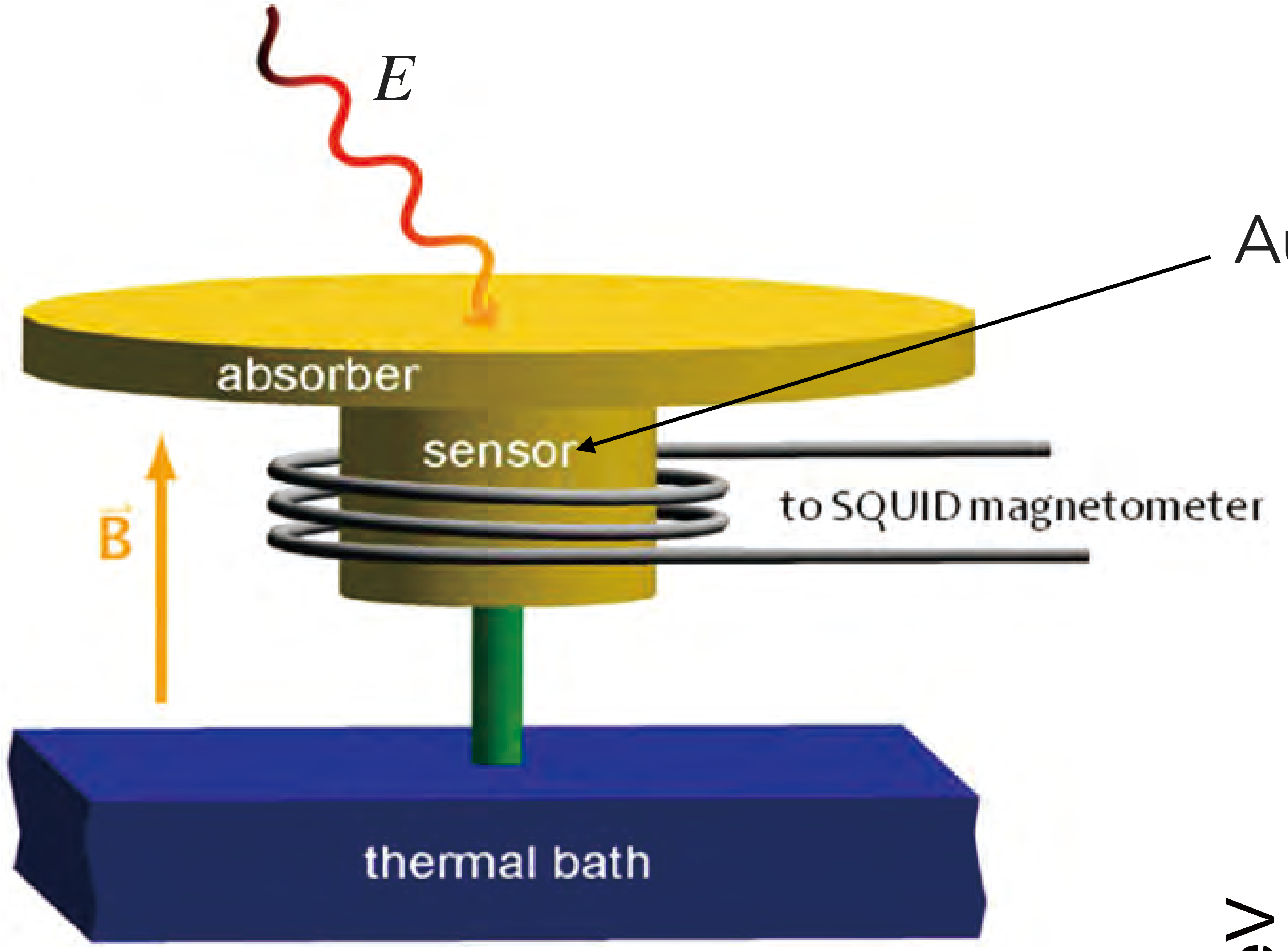

Au:Er 300ppm

Hengstler+ (2015)

$$\delta M = \frac{\partial M}{\partial T}\delta T = \frac{\partial M}{\partial T}\frac{E}{C}$$

$$\Delta E = \sqrt{4k_B T^2 C}\sqrt{2}\left(\frac{\tau_+}{\tau_-}\right)^{1/4}$$

Fleischmann, Enss & Seidel (2005)

τ_+ is a pulse rise time.
A short thermalization time scale is important.

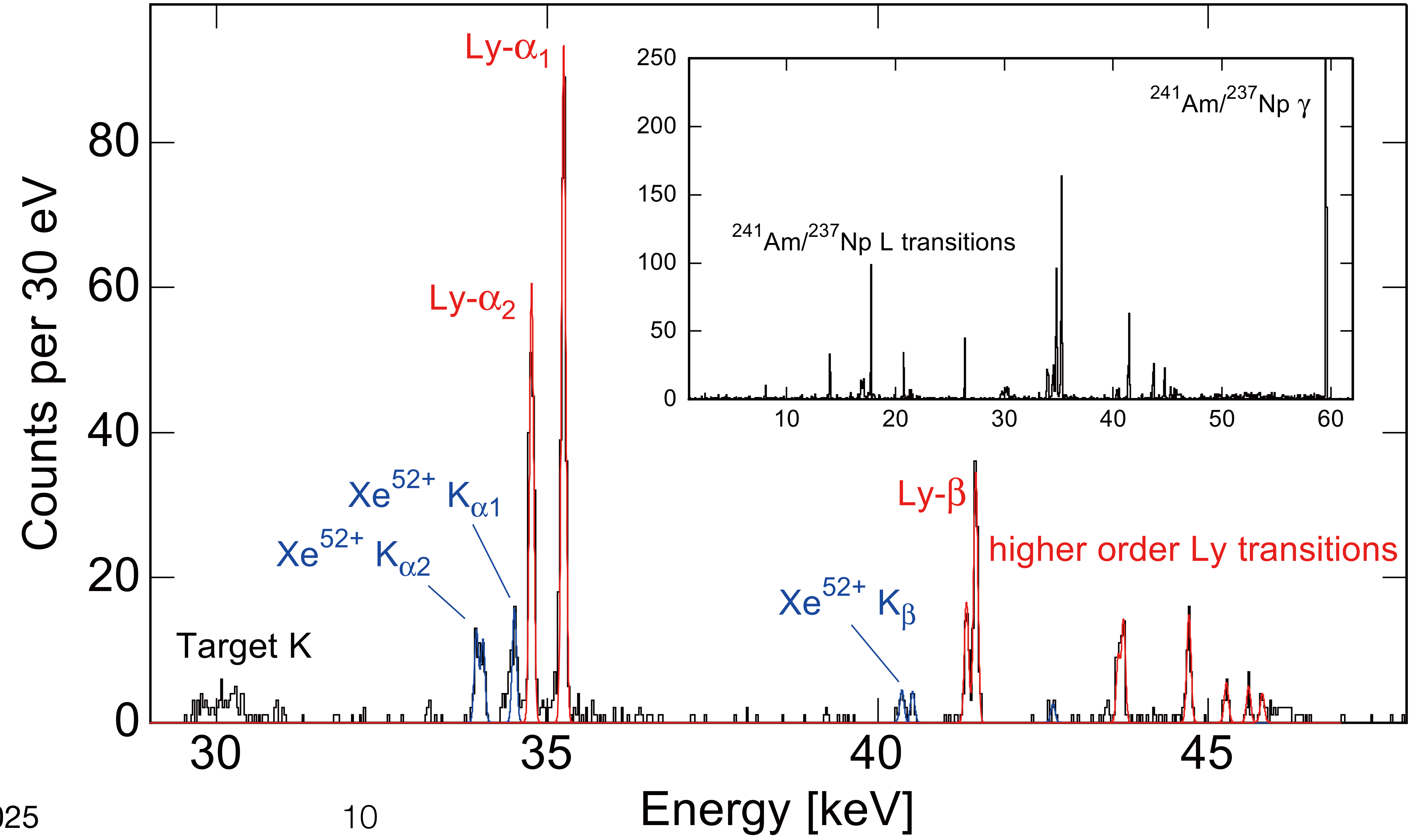

Basics of TES microcalorimeters

TES-type thermometers

- Steep resistance change at a transition edge is utilized as a thermometer.
- Transition temperature can be controlled with
  - Proximity effect: bi or multi-layers of superconductor(s) and normal metals(s), or
  - Magnetic effect: a superconductor doped with a small amount of magnetic material
- The current flow through the TES is controlled with over-etching, normal-conductor banks or bars to control α.

TES example

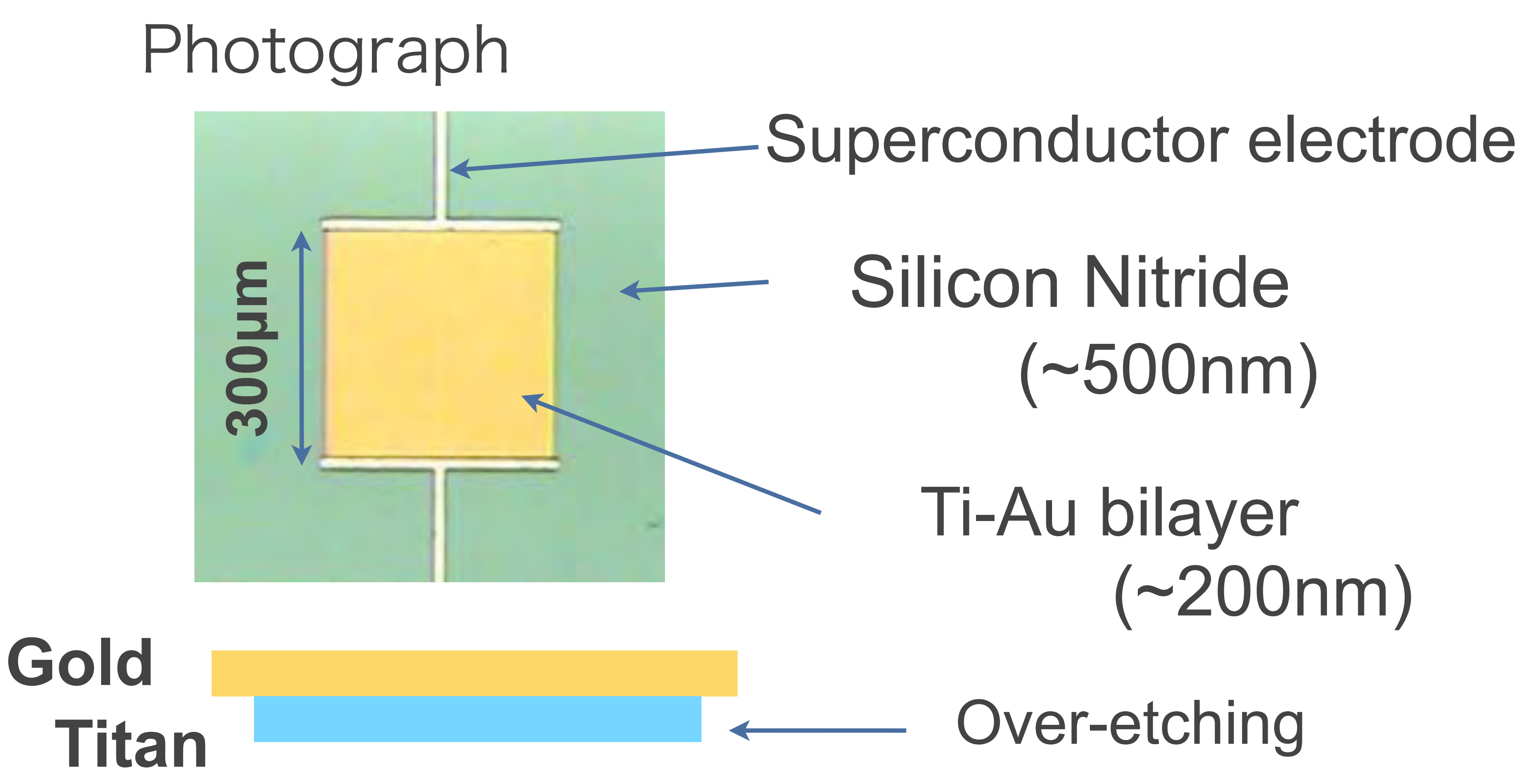

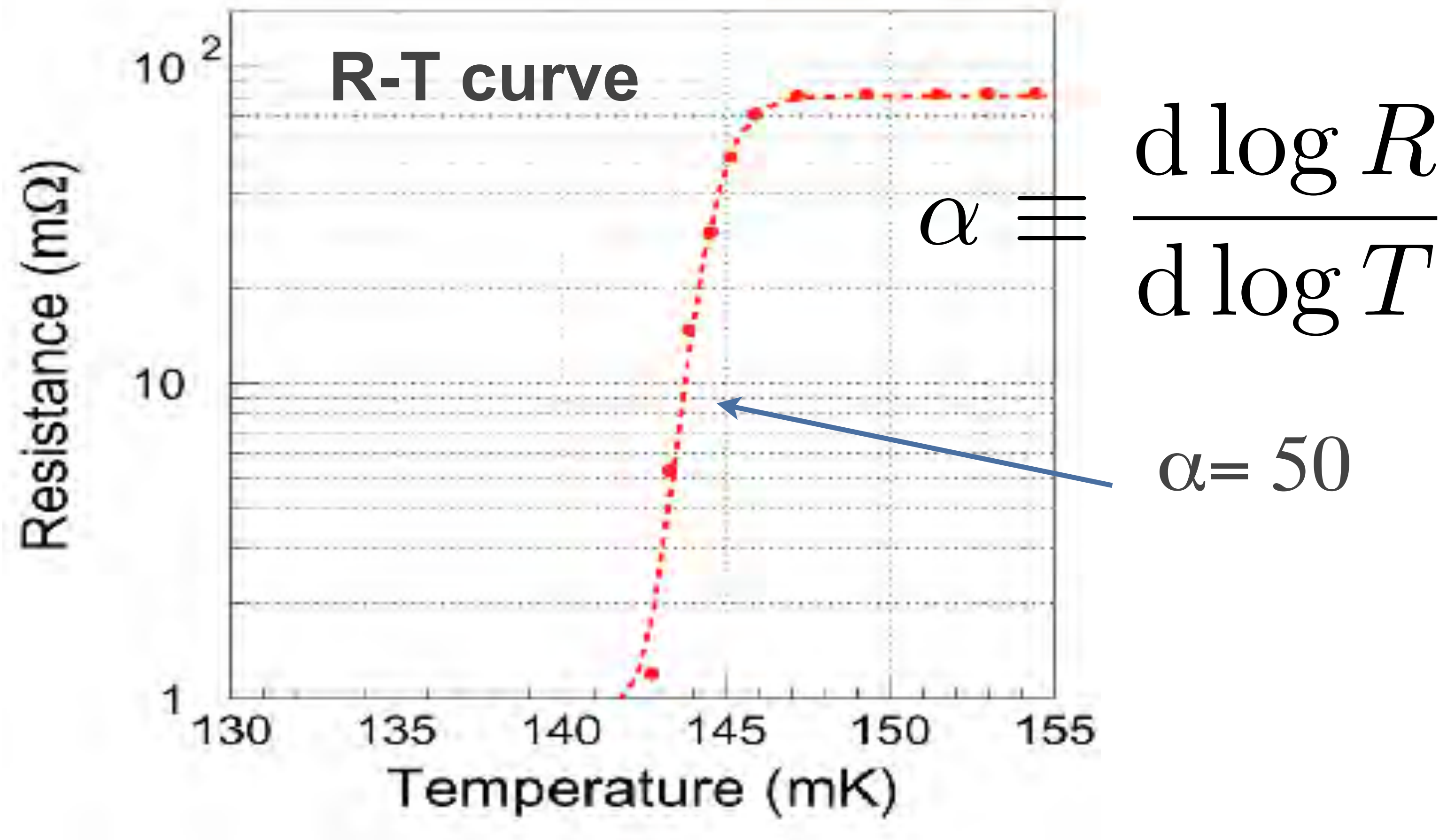

$$\alpha \equiv \frac{\mathrm{d}\log R}{\mathrm{d}\log T}$$

(Strong) Electro-thermal feedback (ETF)

Constant-voltage bias and current readout for TES, since $\alpha > 0$ → Constant current bias and voltage readout are applied to a semiconductor-type thermometer, which also provides ETF.

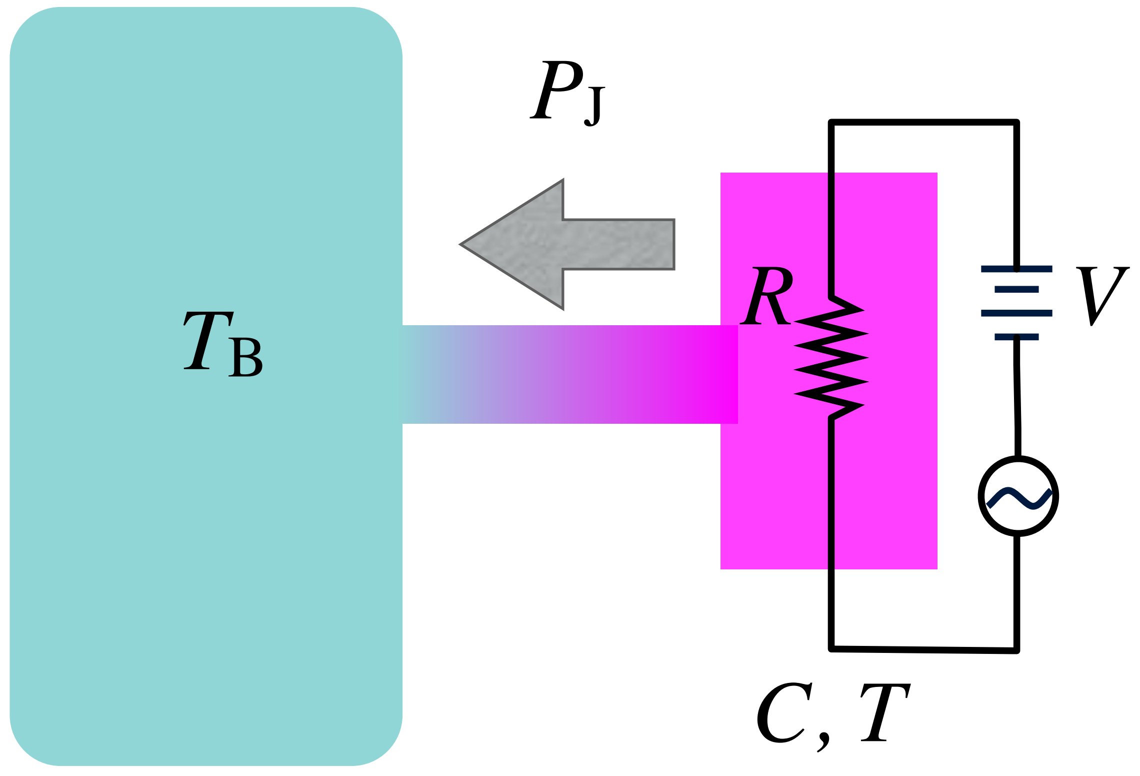

$$P_J = \frac{V^2}{R} \Rightarrow \frac{d\log P_J}{d\log T} = -\alpha \Rightarrow \text{Stable}$$

$\alpha >> 1 \Rightarrow$ Strong feedback

The feedback (ETF) cancels thermal fluctuations from outside, making the device return to the equilibrium temperature with a time scale shorter than the thermal time scale.

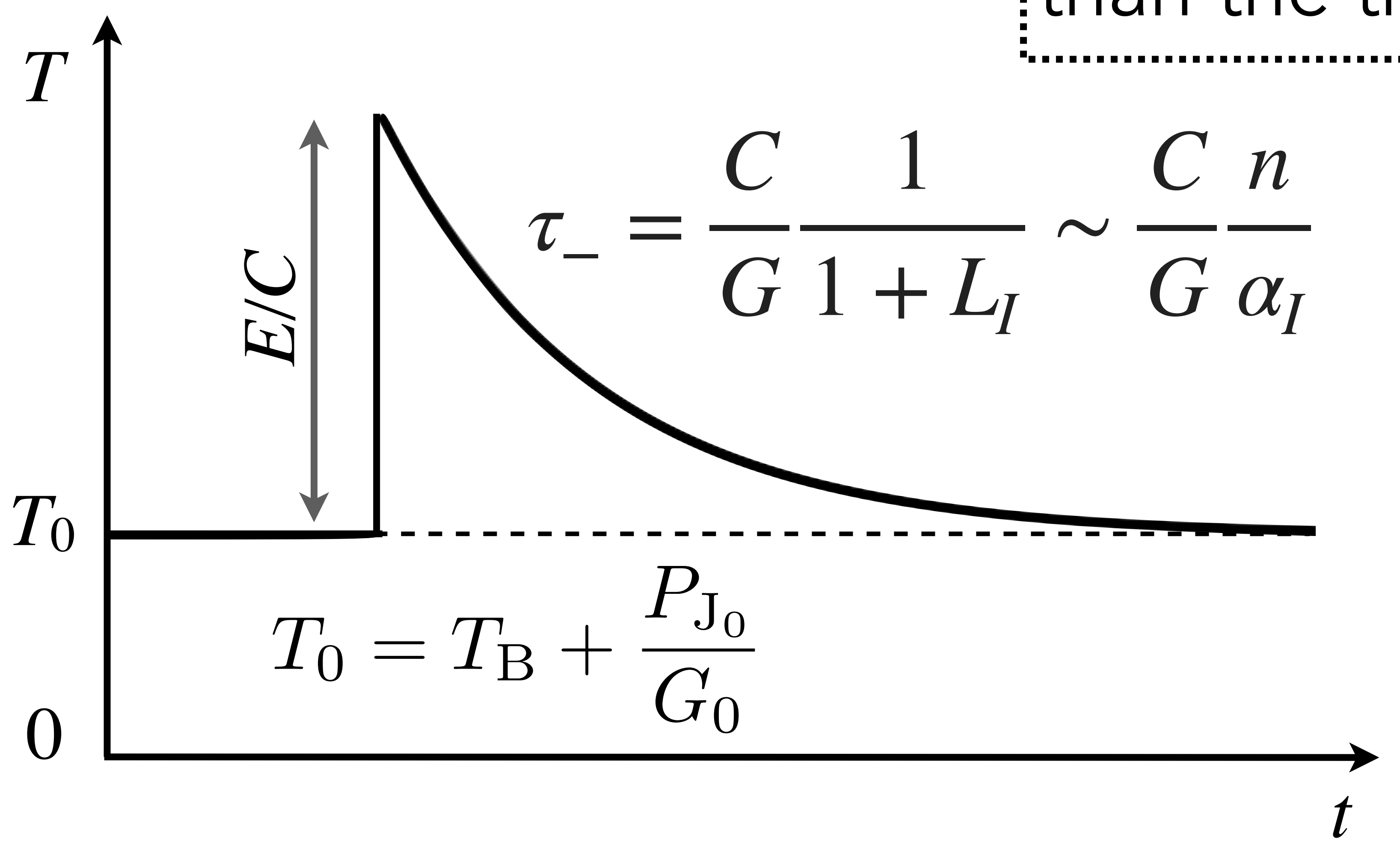

$$\tau_- = \frac{C}{G}\frac{1}{1+L_I} \sim \frac{C}{G}\frac{n}{\alpha_I}$$

$$T_0 = T_B + \frac{P_{J_0}}{G_0}$$

(Heat-dissipating thermometer cases)

Feedback gain $L_I = \frac{P_{J_0}\alpha_I}{GT_0} \sim \frac{\alpha_I}{n}$

$\alpha_I = \alpha$ under constant current

n = Power-law index of thermal link's conductivity $\kappa \propto T^n$

T_0 = Equilibrium temperature

Irwin (1995)

Irwin & Hilton (2005)

IV-curve

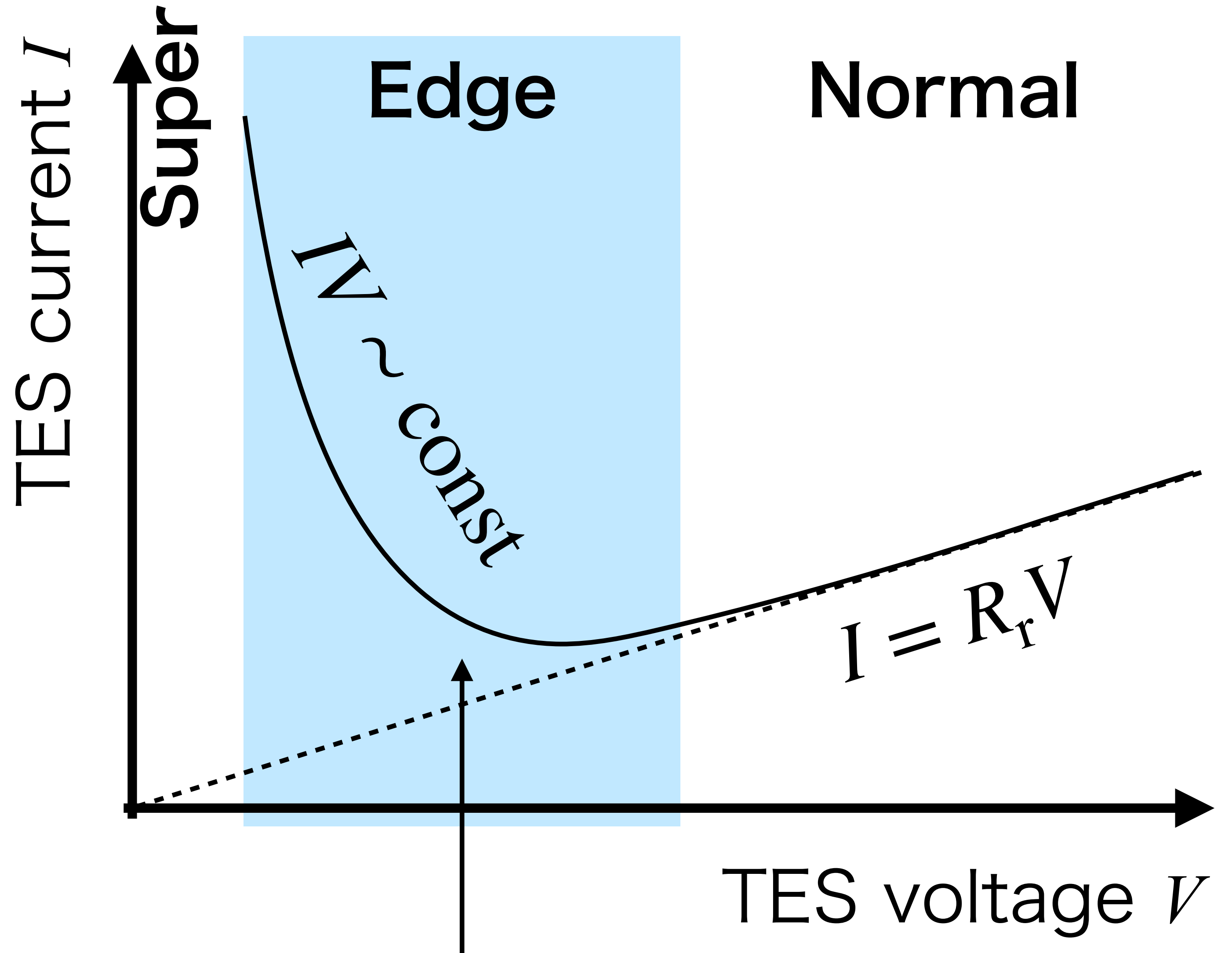

TES can stably operated on the transition edge by the strong ETF.

Best energy determination in linear regime

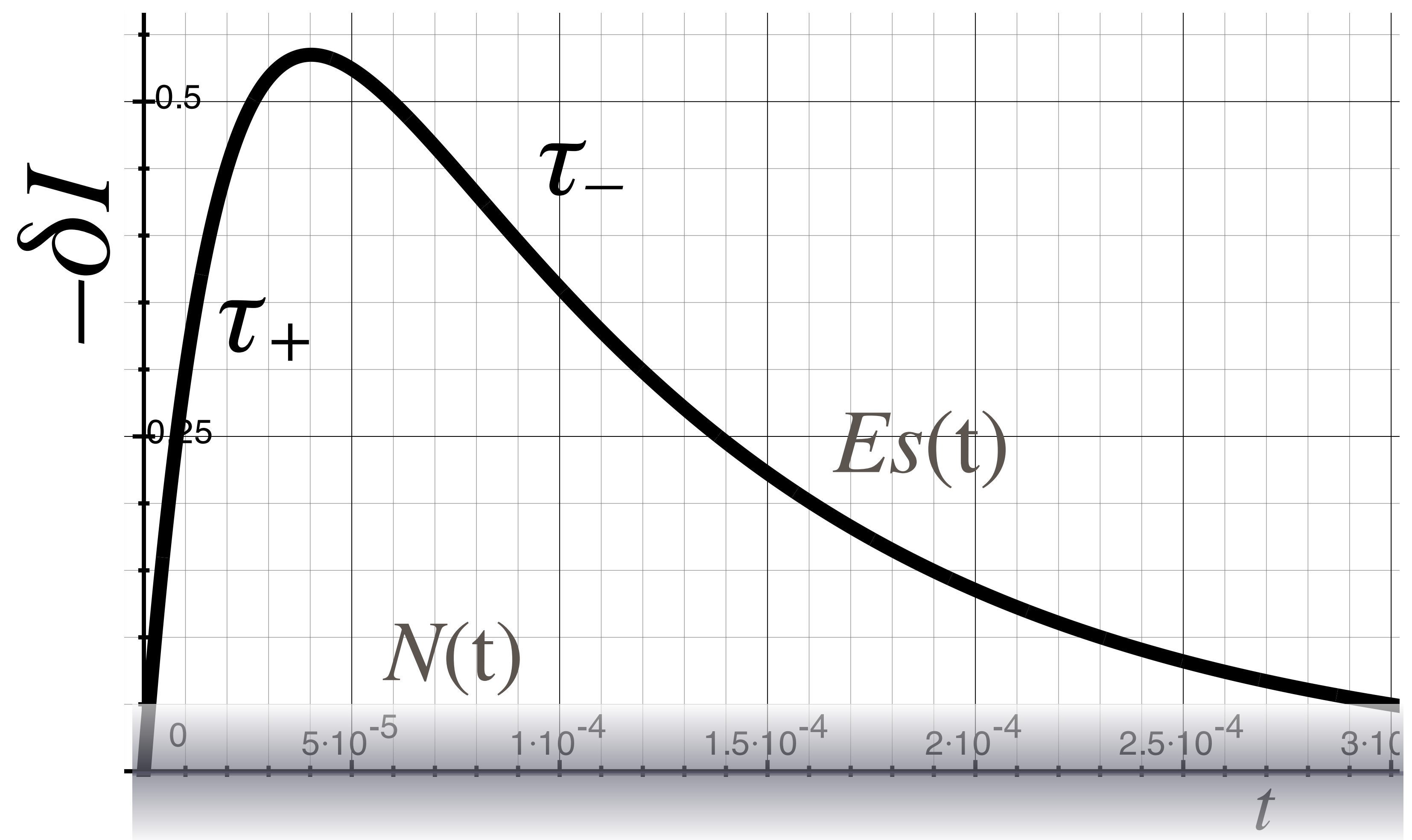

Assumption: $D(t) = Es(t) + N(t)$

$D(t)$: Pulse we observed

$s(t)$: Expected pulse form for a unit input

$N(t)$: Noise that is assumed to be stationary. It can be estimated from data when there is no pulse.

Fourier transforms of the above $D(\omega)$, $s(\omega)$, $N(\omega)$

$s(\omega)$: Responsivity

We perform Bayesian estimation of the value E after $D(t)$ is obtained.

It is reasonable to assume the noise in the frequency domain is Gaussian.
Then, the maximum likelihood is reduced to the minimum χ^2;

$$\chi^2 = \sum_\omega \frac{|D(\omega) - Es(\omega)|^2}{|N(\omega)|^2} \quad \Rightarrow \quad E = 2\pi \sum_t g(t) D(t)$$

$g(t)$ is the inverse Fourier transform of $g(\omega)$

$$g(\omega) = \frac{\dfrac{s(\omega)}{|N(\omega)|^2}}{\sum_\omega \dfrac{|s(\omega)|^2}{|N(\omega)|^2}}$$

Szymkowiak+ (1993)

We call $g(t)$ the pulse template and also the optimal filter.
This is the **Wiener filter** and the denominator is a normalization factor to obtain E.

Energy resolution in linear regime

When you observe an pulse, $D(t)$, the true value of E will be in $\chi^2 \leq \chi^2_{\min} + 1$ with 1-σ probability.

Thus, the FWHM energy resolution is estimated as

$$\Delta E = 2.35\sigma = \frac{2.35}{\sqrt{\sum_\omega \frac{|s(\omega)|^2}{|N(\omega)|^2}}}$$

Using the Noise equivalent power (NEP^2), the above equation is written as

$$\Delta E = \frac{2.35}{\sqrt{\int_0^\infty \frac{4}{NEP^2(\omega)} \frac{d\omega}{2\pi}}}$$

$$NEP^2 \equiv \frac{PSD_N(\omega)}{|s(\omega)|^2}$$

" $\sum_\omega$ " means " $\sum_{\omega=-\infty}^{\infty}$ " while PSD is defined in $\omega \geq 0$. Thus

$$PSD_N(\omega) = \frac{2}{T}|N(\omega)|^2 \qquad d\omega = \frac{2\pi}{T} \qquad \sum_{\omega=-\infty}^{\infty} = 2\int_0^\infty$$

T is the pulse record length

Szymkowiak+ (1993)
Moseley, Mather, & McCammon (1984)

NEP of an ideal detector in the linear regime

Three inevitable noise sources:

- **Phonon noise**: random thermal flow through the thermal link causes this noise.
- **Johnson noise**: Thermal noise across the thermistor resistance. Here, we ignore the current dependence of the resistance.
- **Readout noise**: For TESs, the thermal noise across the SQUID shunt resistance dominates.

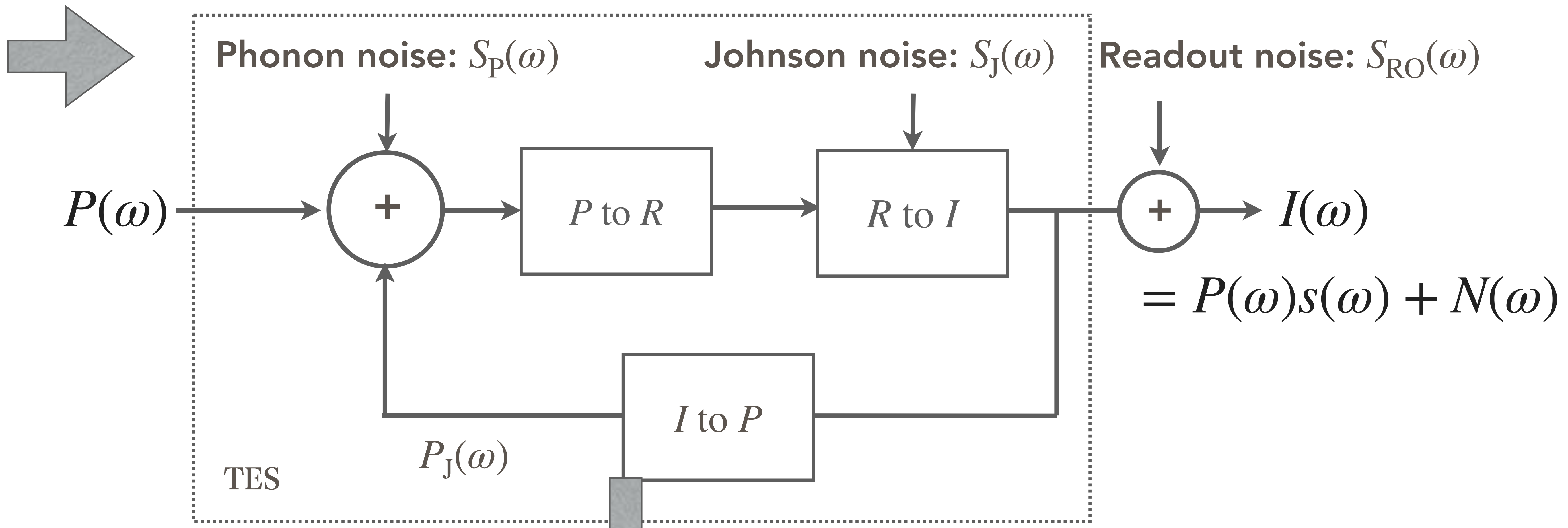

- For $\omega < 1/\tau\_$, phonon noise dominates, and NEP is independent of ω and α;

$NEP^2(\omega) = 4k_B T_0^2 G F(T_0, T_B)$, where

$$F(T_0, T_B) = \frac{n+1}{2n+3}\frac{(T_0/T_B)^{2n+3}-1}{(T_0/T_B)^{n+1}-1} \sim \frac{1}{2}$$ for typical T_0/T_B and n.

Mather (1982)

- For $\omega > 2\pi/\tau\_$, Jonson noise dominates, and NEP rapidly increases with increasing ω.

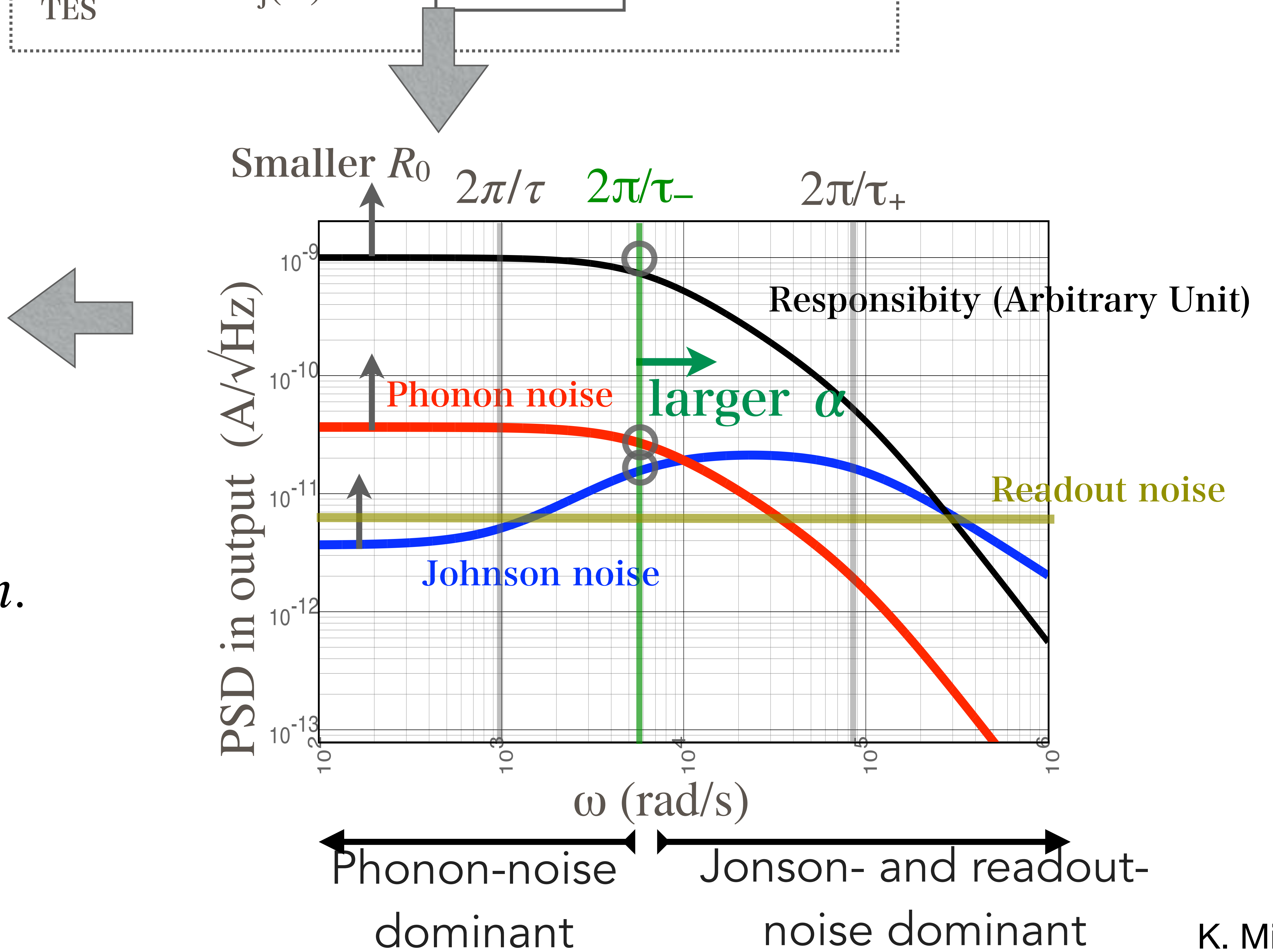

Energy resolution of an ideal detector in the linear regime

Neglecting the readout noise and taking F=1/2, we obtain,

$$\Delta E = \frac{2.35}{\sqrt{\int_0^\infty \frac{4}{NEP^2(\omega)} \frac{d\omega}{2\pi}}} = 2.35\sqrt{4k_B T_0^2 C \frac{\sqrt{n/2}}{\alpha_I}}$$

NEP² @low fr. $4k_B T_0^2 G$

1/ (bandwidth) $\frac{C}{G}\frac{n}{\alpha}$

$$\frac{1}{\int_0^\infty \frac{4}{NEP^2(\omega)} \frac{d\omega}{2\pi}} \sim \frac{NEP^2(\omega < 1/\tau_-)}{4} \times \tau_-$$

I often hear, "By making α larger, you can obtain better energy resolution."

The statement is not applicable in many cases and thus is very misleading.

There is another important factor in TES; non-linearity in response.

Non-linearity of response

Source of non-linearity	Semiconductor	TES	MMC
Temperature dependence of heat capacity	small effect	small effect	small effect
Imperfect constant bias	large effect, can be partly corrected for	large effect, can be partly corrected for	not applicable
Nonlinear response of thermometer	Significant effect	Large effect: signal saturates	Small effect

↓ Good linearity

e.g. Fleischmann, Enss & Seidel (2005)

Response to high-energy X-rays of TES for STEM EDS

TES μ-calorimeter is designed for ≤ 10 keV, i.e., $E_{\mathrm{sat}} = 10\ \mathrm{keV}$

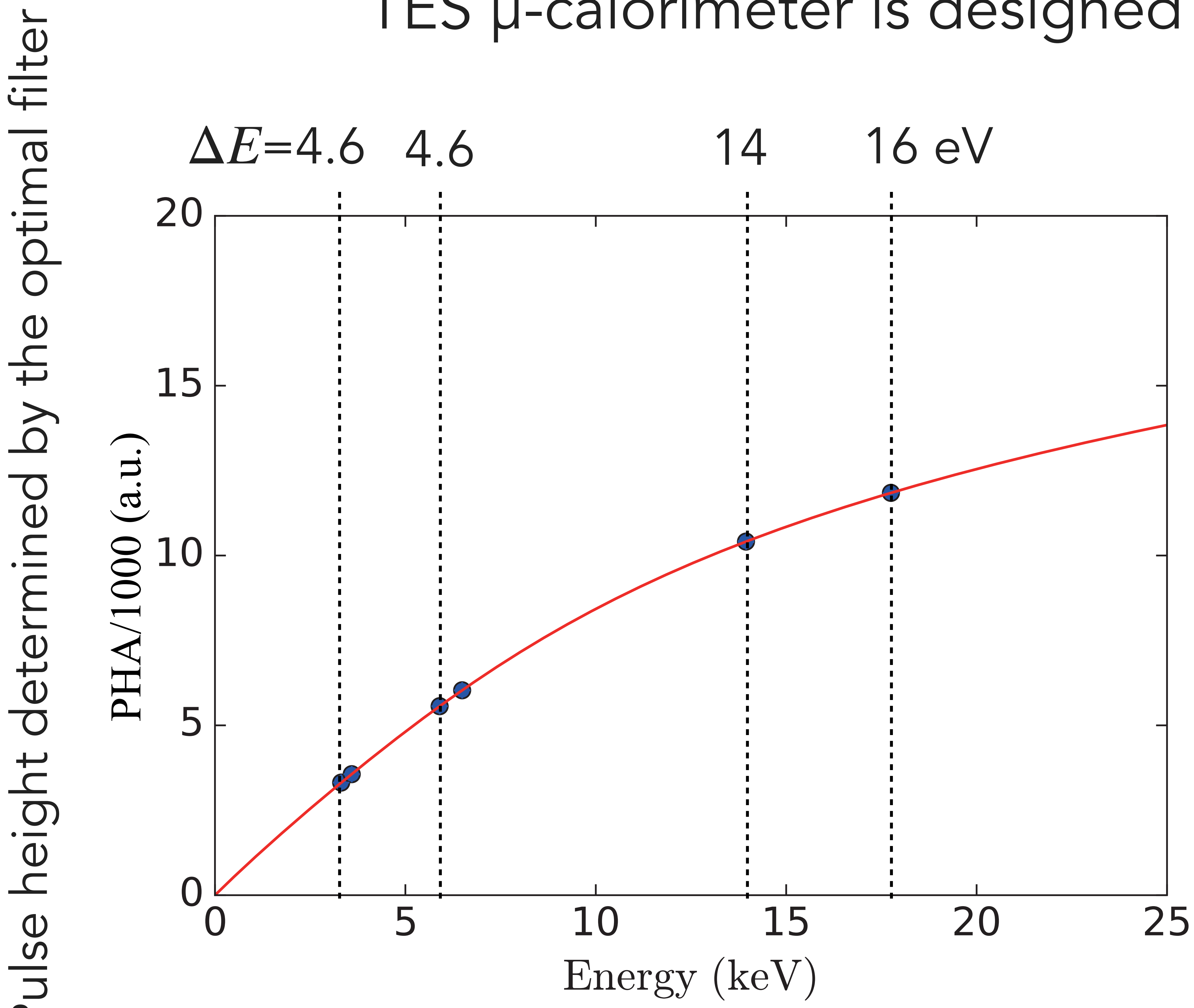

Incident X-ray energy

Note: Even ≤10 keV, the response was not linear at a % level.
Thus, precise calibration was necessary.

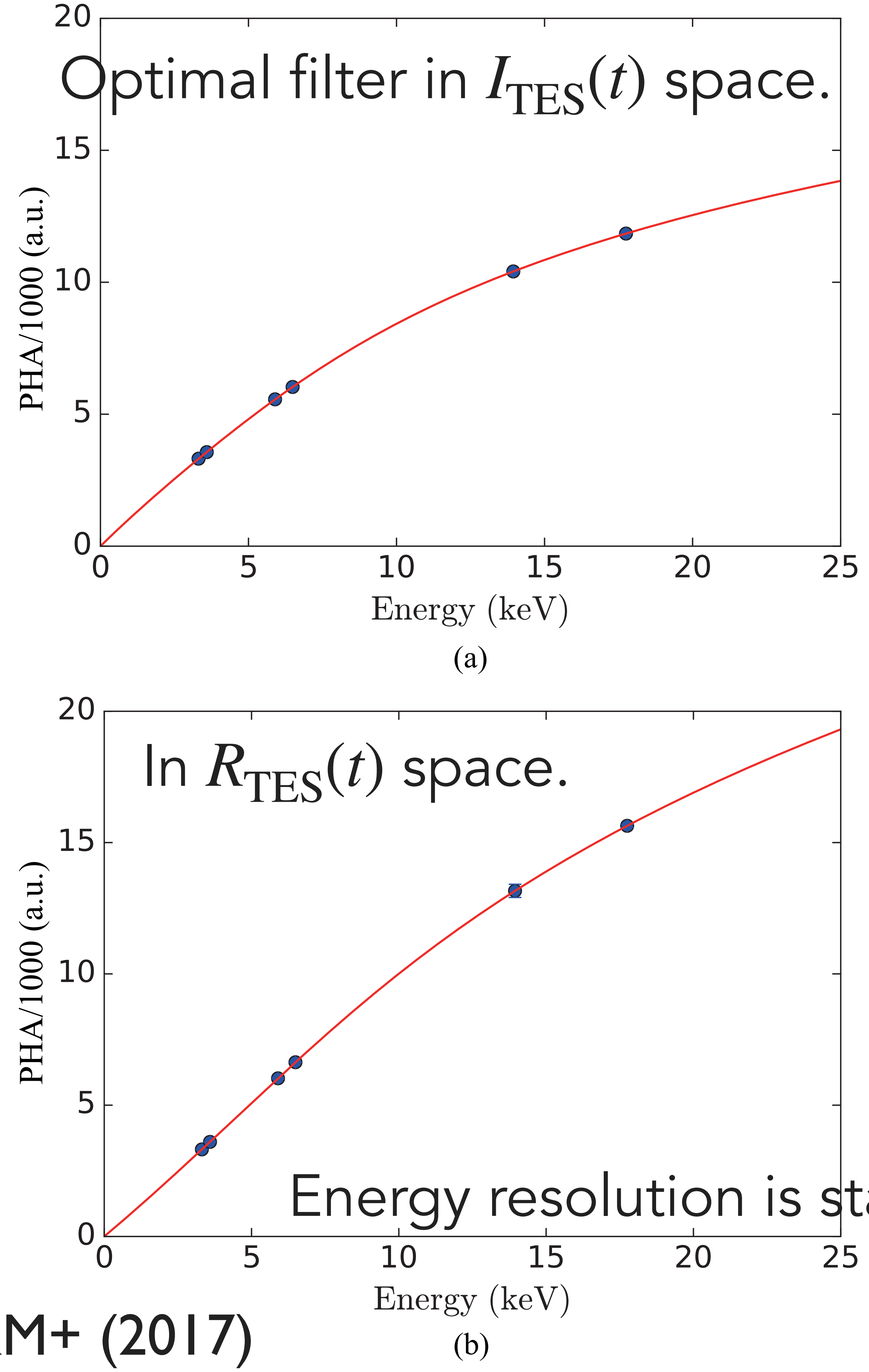

Energy resolution is stay same.

- Pseudo-constant bias with a shunt resistor.
- $I_{\mathrm{TES}}(t)$ is read by SQUIDs.

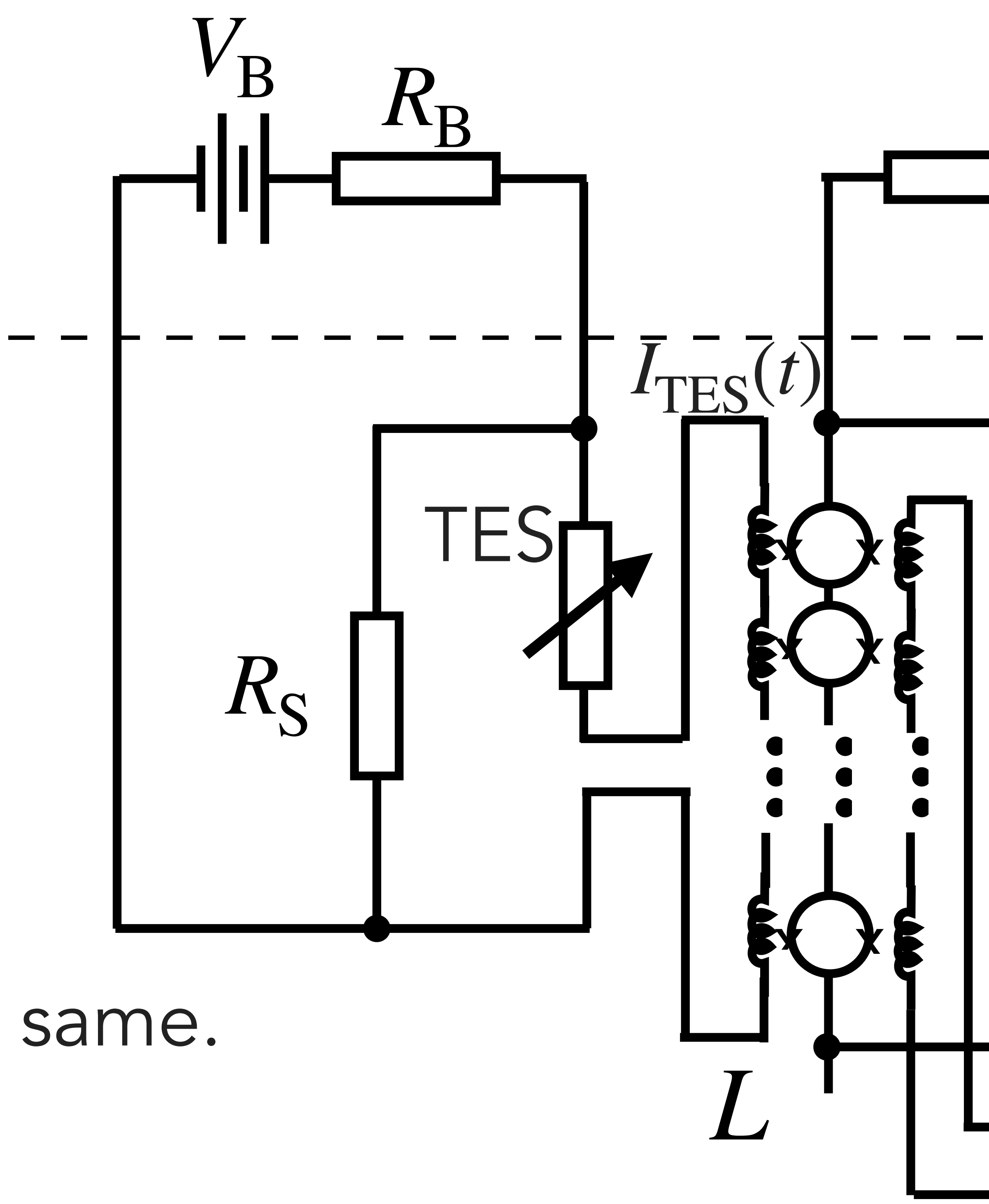

Muramatsu,.. KM+ (2017)

Simple TES saturation model

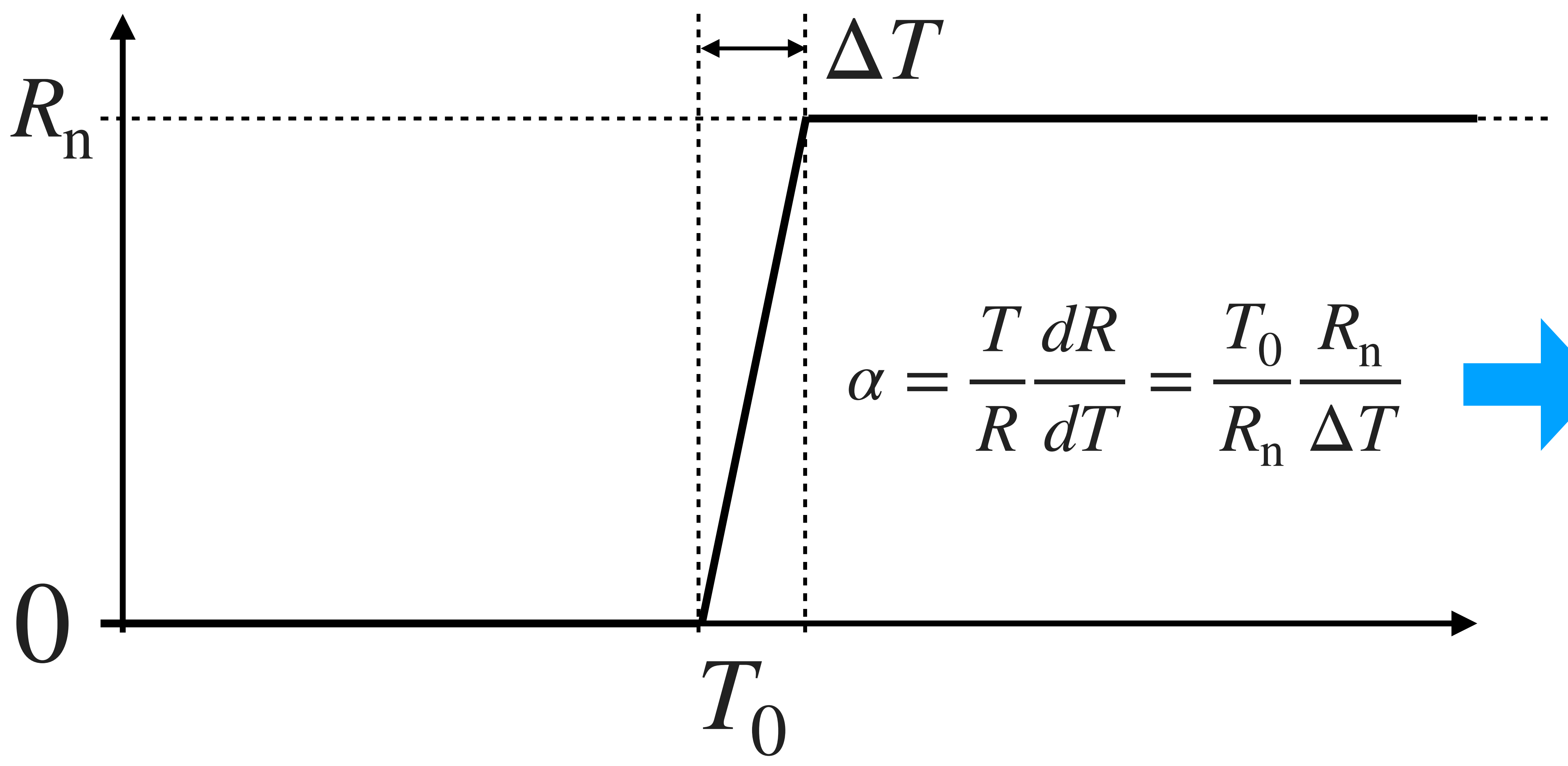

$$\alpha = \frac{T}{R}\frac{dR}{dT} = \frac{T_0}{R_n}\frac{R_n}{\Delta T} \Rightarrow \Delta T = \frac{T_0}{\alpha}$$

TES microcalorimeters

$$E_{\rm sat} = C\Delta T = \frac{CT}{\alpha}$$

Key design parameters

TES microcalorimeters
Energy resolution
$\Delta E = 2.35\sqrt{4k_B T^2 C \frac{\sqrt{n/2}}{\alpha}} = 2.35\sqrt{4k_B T E_{\rm sat}\sqrt{n/2}}$
Pulse decay time
$\tau_- = \frac{Cn}{G\alpha} = \frac{E_{\rm sat} n}{GT}$
Saturation energy
$E_{\rm sat} = \frac{CT}{\alpha}$

- Once you fix the maximum energy you want to detect, i.e., $E_{\rm sat}$, the energy resolution is determined only by the temperature, T, while response time by T and G.
- High energy resolution and fast response are contradictory requirements for T.

Mitsuda (2016)

Response time does not matter for most astronomy applications, but for ground applications, fast response is sometimes essential.

TES microcalorimeter array for STEM EDS (Material science)

- Requirements
  - Counting rate: >5 kcps
  - Energy range: 0.5 – 10 keV
  - Energy resolution: FWHM < 10 eV @ 6 keV
- Design solution
  - 8x8 format, 64-pixel TES microcalorimeter
  - The relatively high transition temperature of ~150mK for a fast response
    - ~600 cps/pixel (c.f. ~300 cps/pixel if 100mK)

- Detector developed

Fabricated in house using the ISAS/JAXA nano clean room

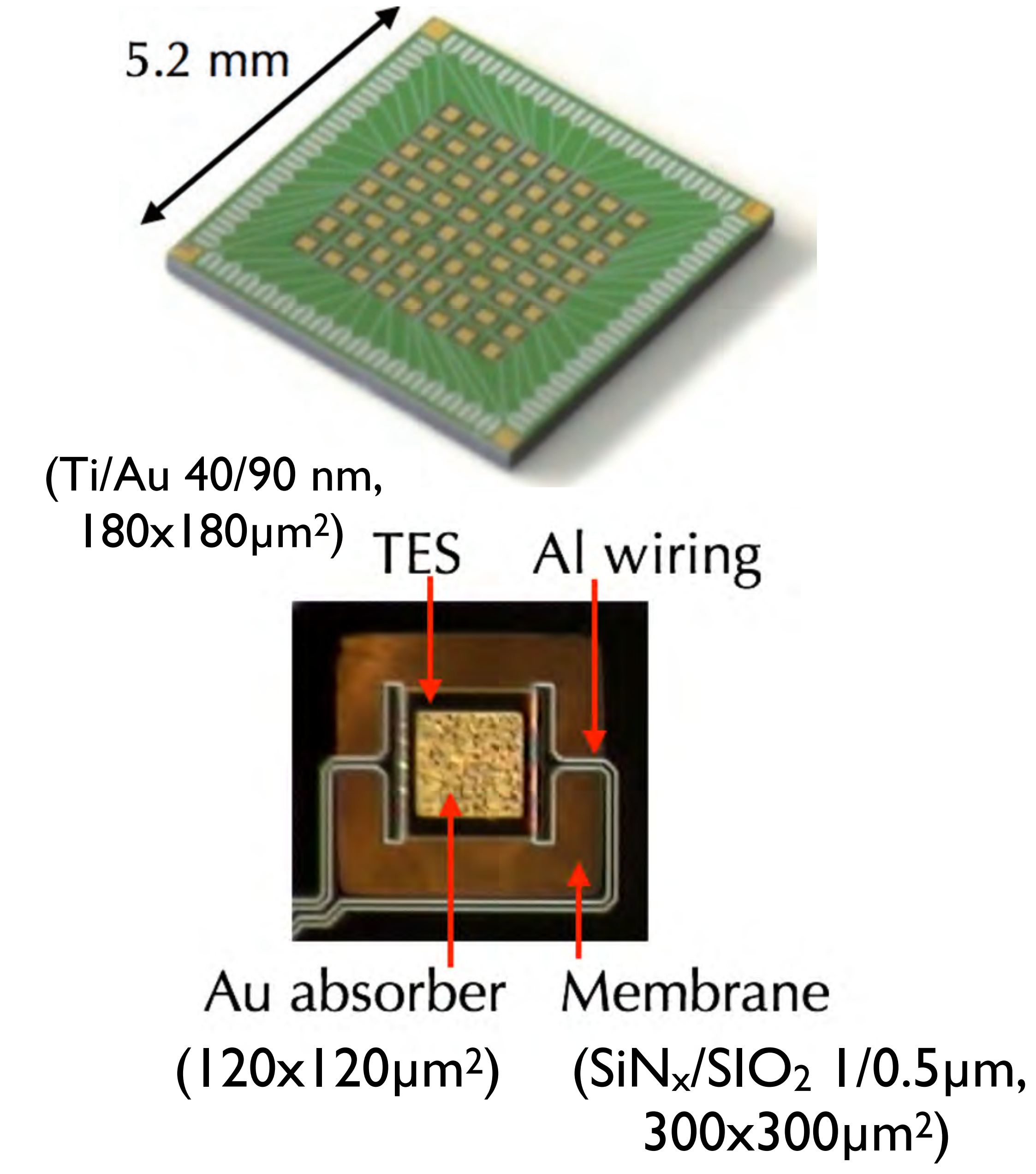

Fast response: proved

Transition T = 162 mK
Pulse decay =70μs

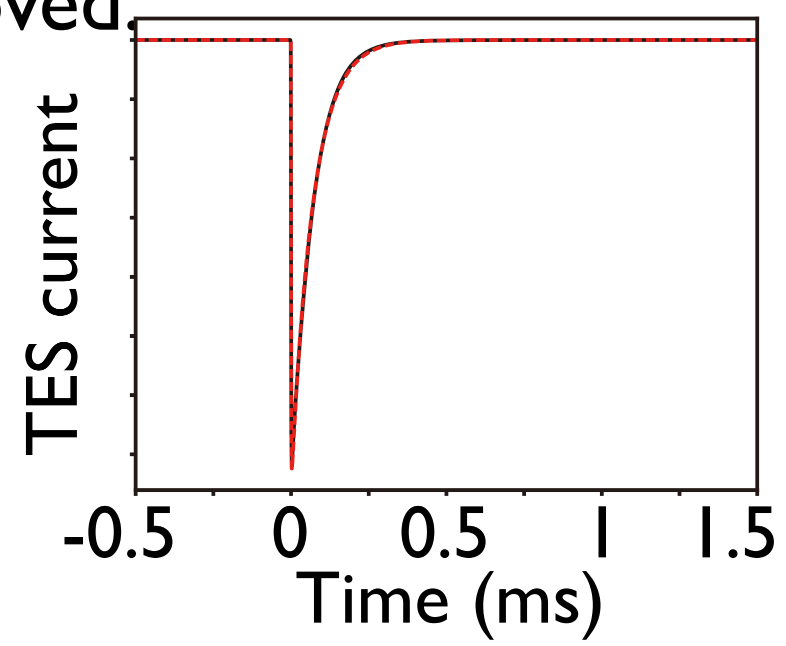

FWHM<10 eV energy resolution: proved.

4.9 eV at 5.9 keV at JAXA labo environment

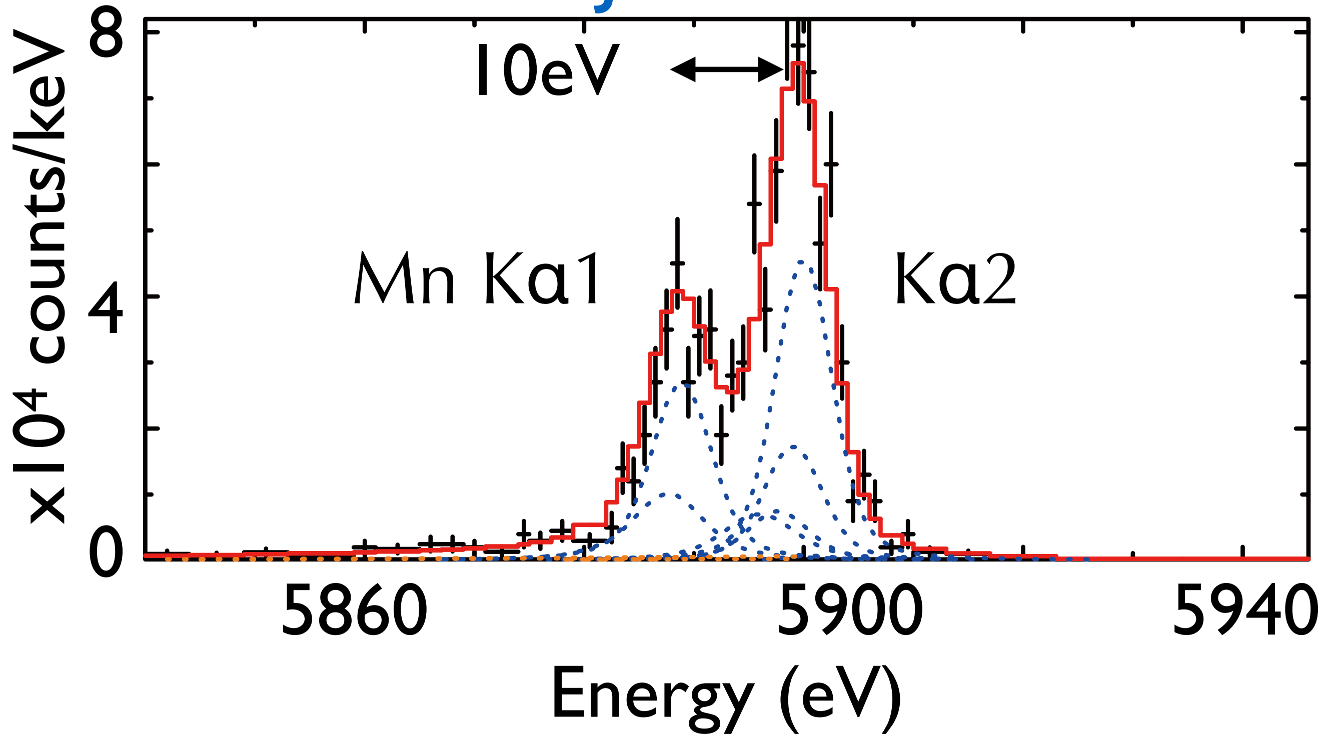

Muramatsu, .. KM+ (2016)

Processes to make TES μ-calorimeters at ISAS/JAXA clean room

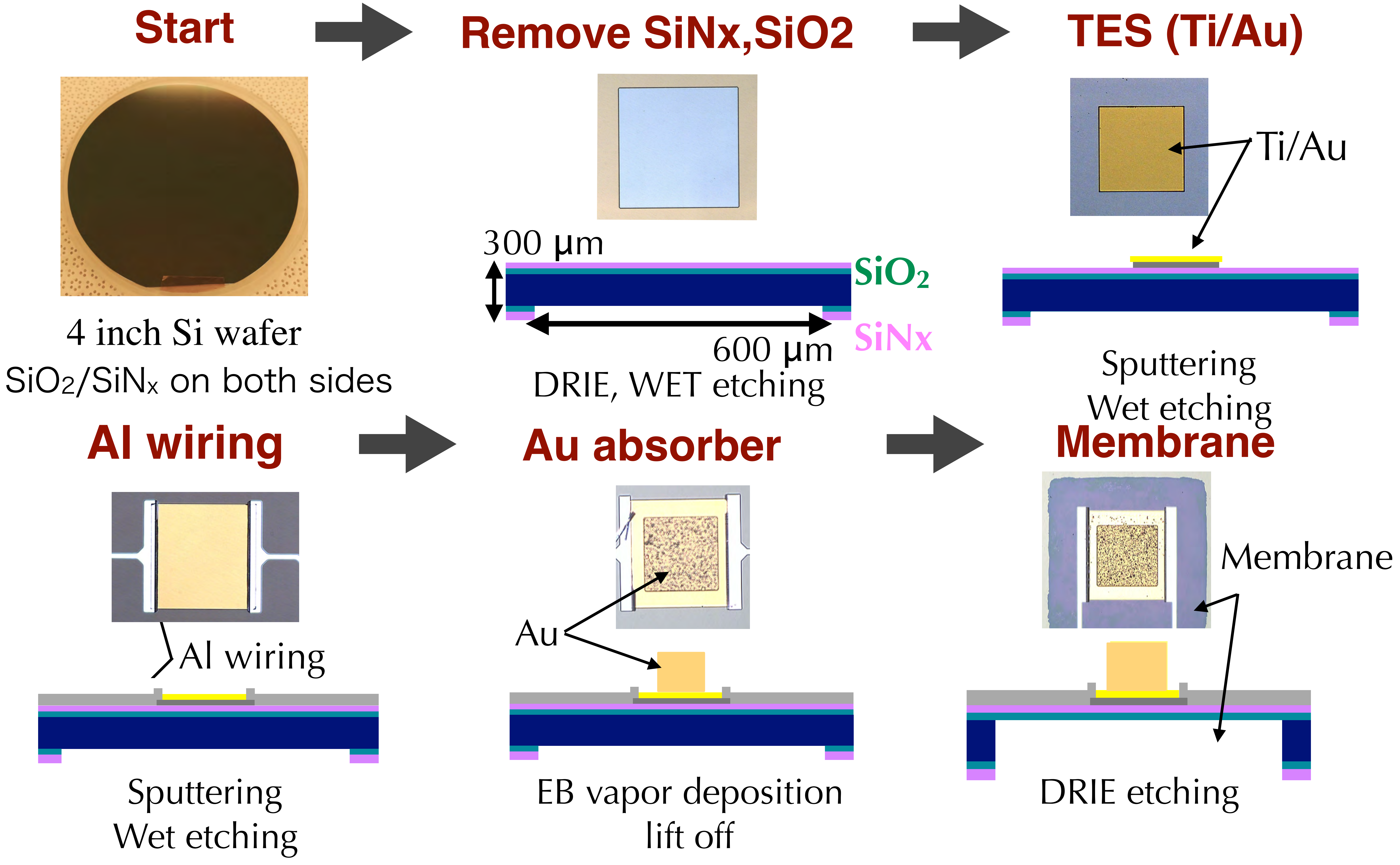


TES membrane sputtering


Al sputtering deposition


Photo mask alignment


EB vapor deposition


Wet etching

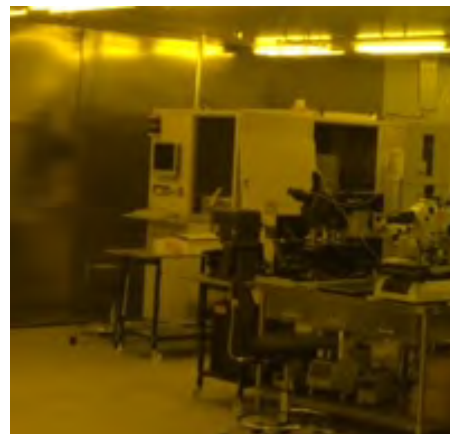
Dry etching (ICP, DRIE)

TES microcalorimeter array for STEM EDS (Material science)

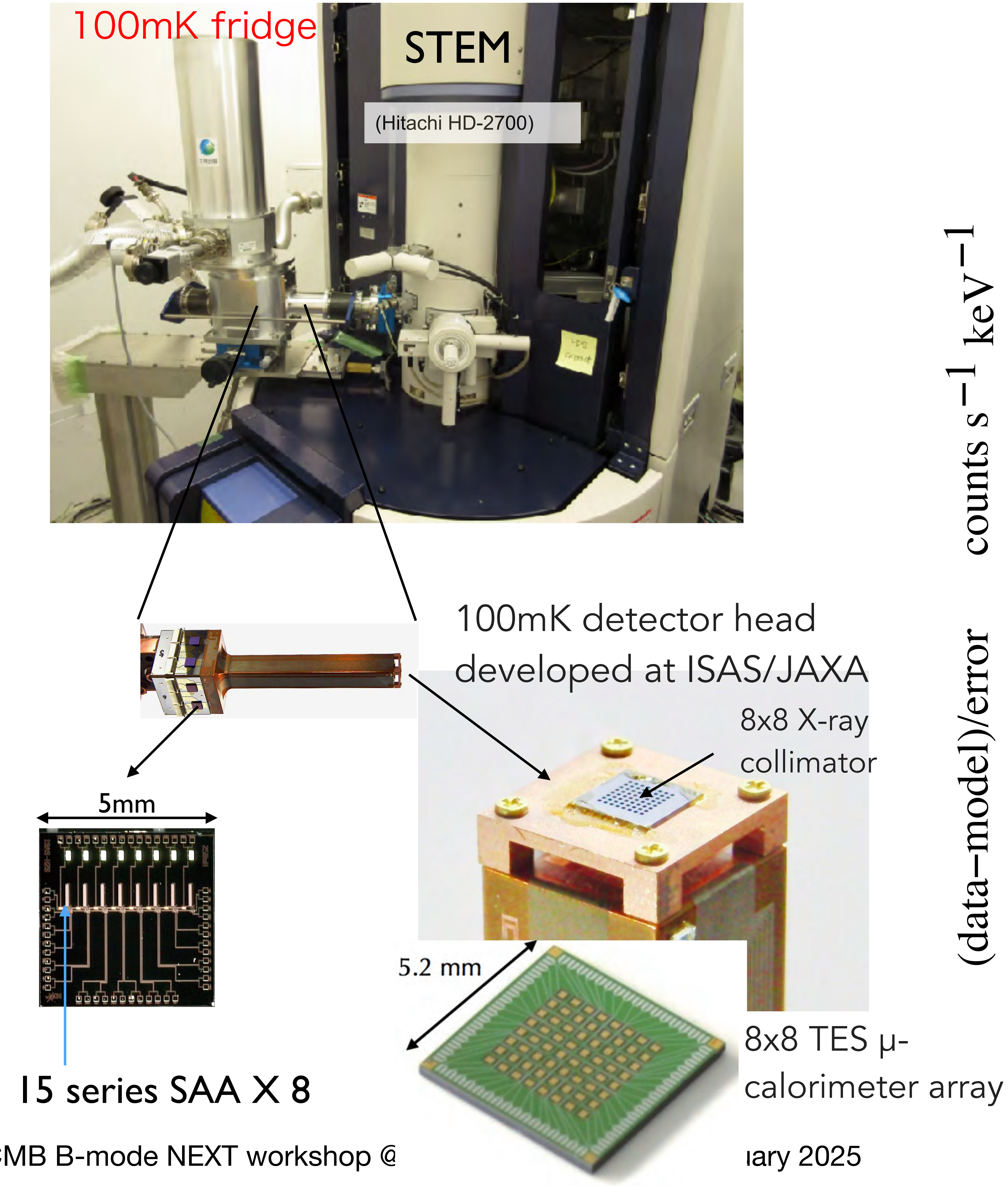

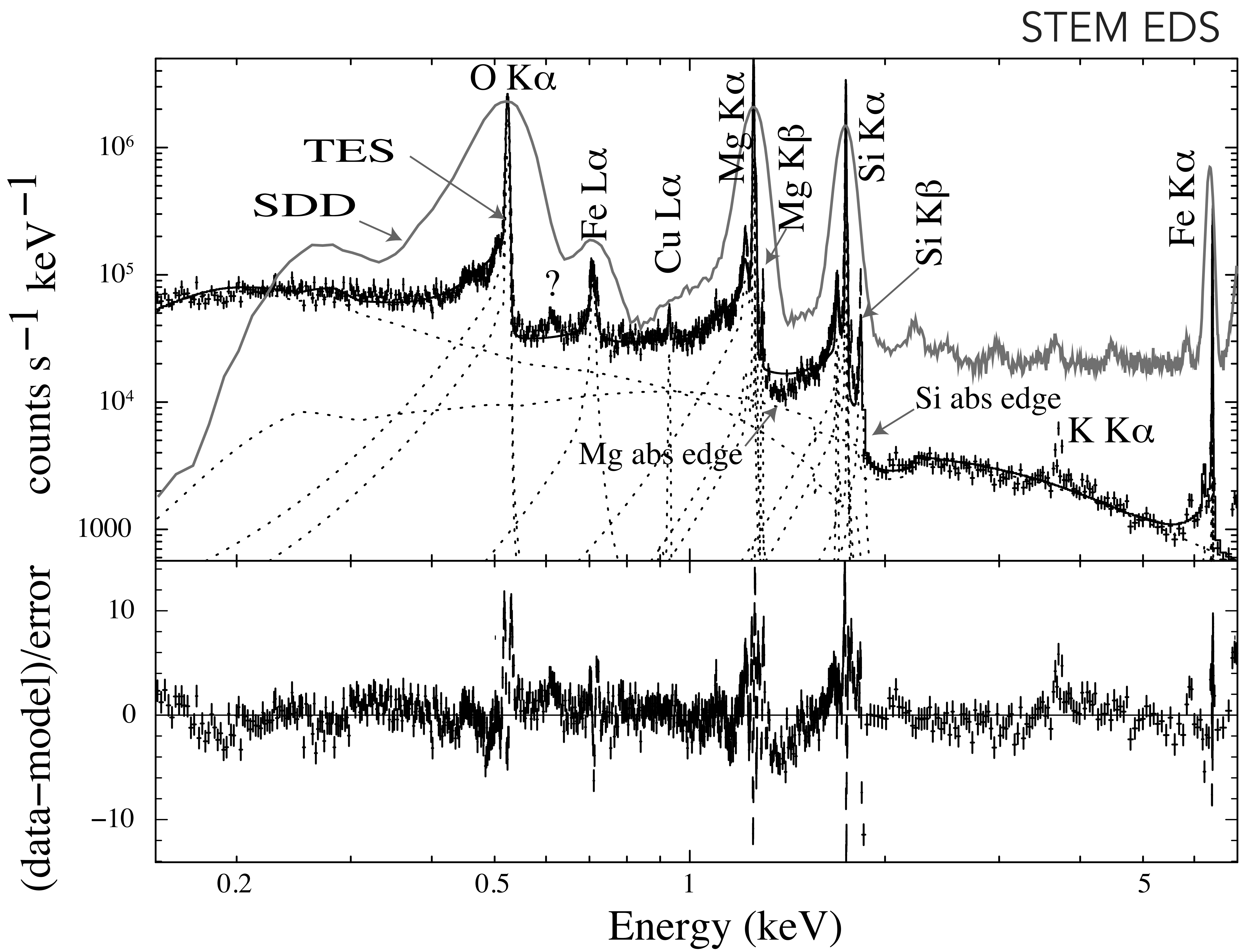

Hayashi (2019)
Hayashi, .. KM + (2018)

Basics of TES bolometers

Bolometers

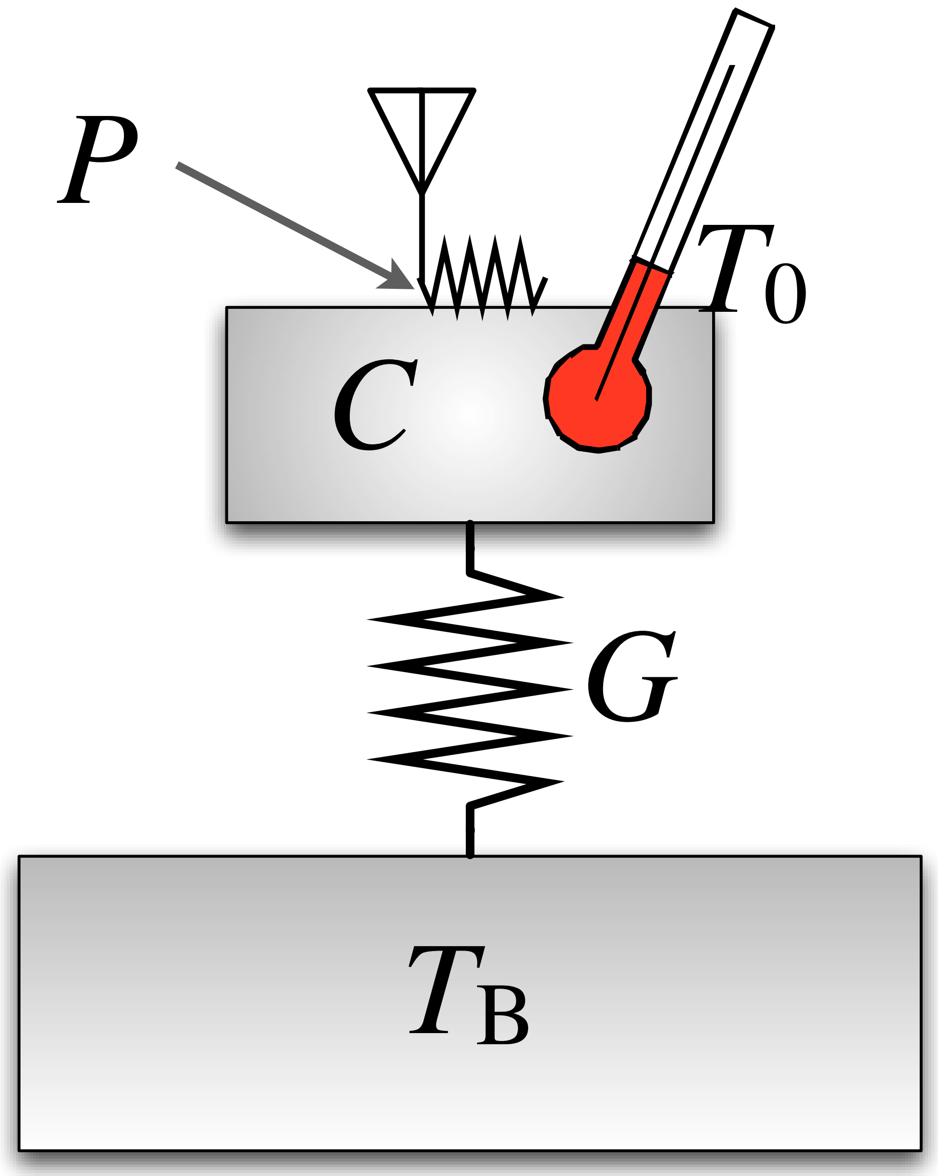

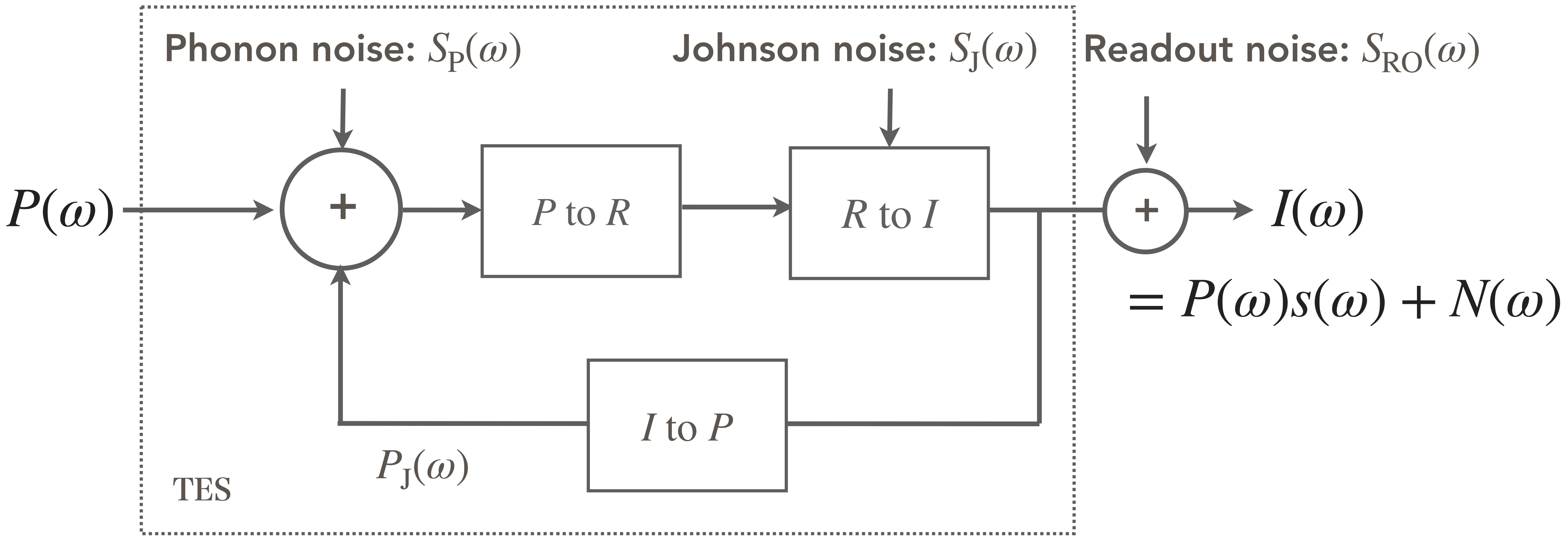

Key performance parameters

- Noise equivalent power
  - $NEP^2(\omega) = 4k_B T_0^2 G F(T_0, T_B)$, where

$$F(T_0, T_B) = \frac{n+1}{2n+3} \frac{(T_0/T_B)^{2n+3} - 1}{(T_0/T_B)^{n+1} - 1} \sim \frac{1}{2}$$ for typical T_0/T_B and n.

- Usable Frequency range
  - $\omega < 2\pi/\tau_-$, where $\tau_- = \dfrac{C}{G}\dfrac{1}{1+L_I} \sim \dfrac{C}{G}\dfrac{n}{\alpha_I}$

We have already seen those equations in the TES microcalorimeter section.

Simple TES saturation model

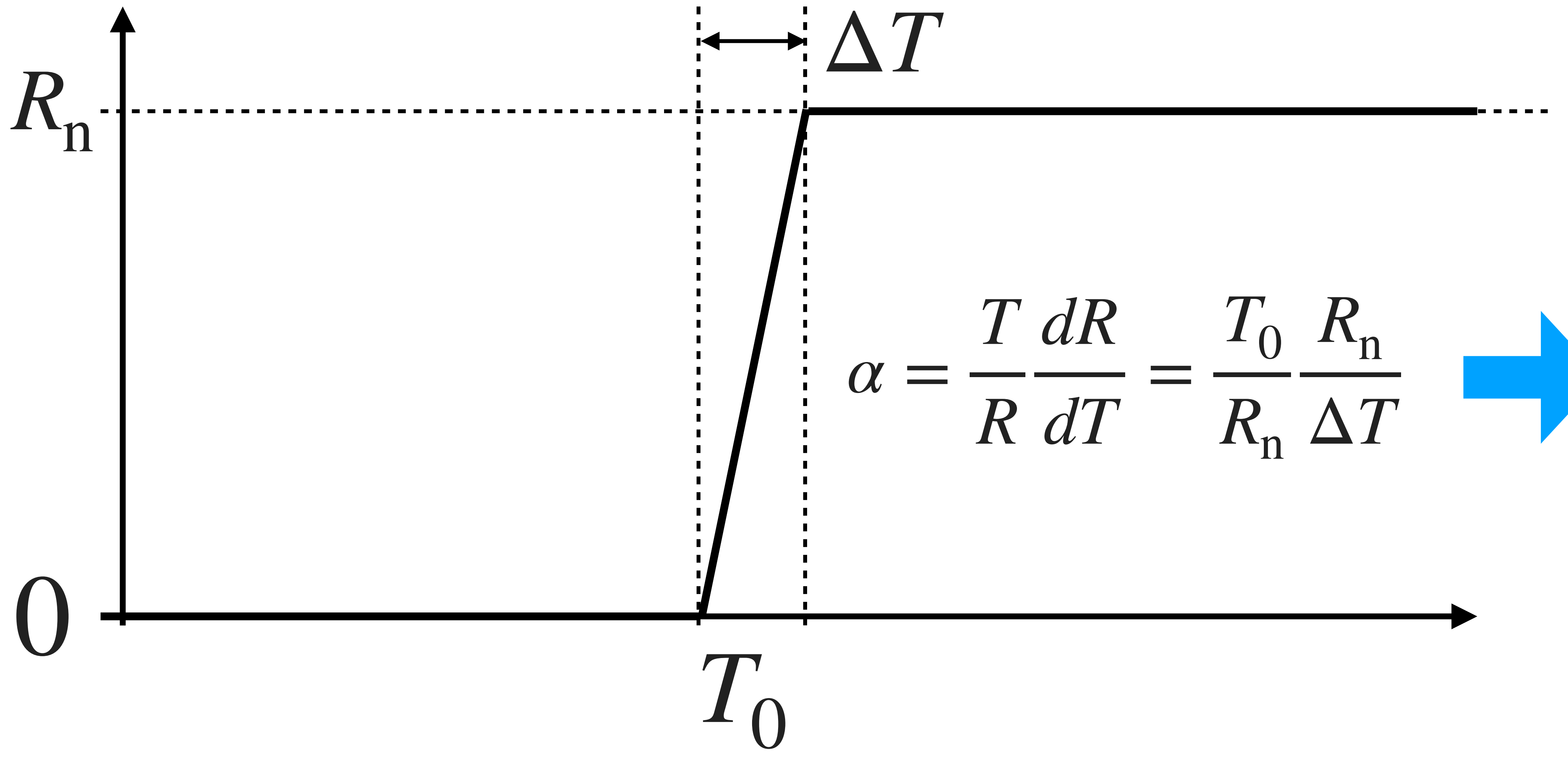

$$\alpha = \frac{T}{R}\frac{dR}{dT} = \frac{T_0}{R_n}\frac{R_n}{\Delta T} \Rightarrow \Delta T = \frac{T_0}{\alpha}$$

TES microcalorimeters

$$E_{sat} = C\Delta T = \frac{CT}{\alpha}$$

TES bolometers

$$P_{sat} = G\Delta T = \frac{GT}{\alpha}$$

Key design parameters

TES microcalorimeters	TES bolometers
Energy resolution $$\Delta E = 2.35\sqrt{4k_\mathrm{B}T^2C\frac{\sqrt{n/2}}{\alpha}} = 2.35\sqrt{4k_\mathrm{B}TE_\mathrm{sat}\sqrt{n/2}}$$	Noise equivalent power $$NEP^2 = 2k_\mathrm{B}T^2G = 2k_\mathrm{B}TP_\mathrm{sat}\alpha$$
Pulse decay time $$\tau_- = \frac{Cn}{G\alpha} = \frac{E_\mathrm{sat}n}{GT}$$	Detector response time $$\tau_- = \frac{Cn}{G\alpha} = \frac{CTn}{P_\mathrm{sat}\alpha^2}$$
Saturation energy $$E_\mathrm{sat} = \frac{CT}{\alpha}$$	Saturation power $$P_\mathrm{sat} = \frac{GT}{\alpha}$$

We set $F(T_0, T_\mathrm{B}) \sim \frac{1}{2}$.
We simply denote T_0 as T, and α_I as α.

- Once you fix the maximum power you need to accept, i.e., P_sat, the NEP is determined by T and α.
- You obtain a better NEP with smaller α. However, it should be noted that the above equations hold for $\alpha \gg 1$.
- The advantages of TES over semiconductor-type are the wider frequency range (the fast response) and signal multiplexing.

Example application, which I am interested in now:

0-th order design study of the new TES bolometers for non-astronomy application

Example design of the TES bolometer for non-astronomy application

- Key requirements
  - Noise equivalent power: $\sqrt{NEP^2} = 2 \times 10^{-17}$ W Hz$^{-1/2}$
  - Highest frequency = 125 kHz, i.e., fastest response time: $\tau_- = 8\ \mu$s
  - Maximum signal: $P_{\mathrm{sat}} = 1 \times 10^{-11}$ W
- Boundary condition
  - The power is resistively dissipated near the TES.

- For most astronomy applications, NEP is the most important requirement.
- However, in the above example, the frequency range and the maximum signal are stringent requirements.

TES bolometer with resistive heat dissipation

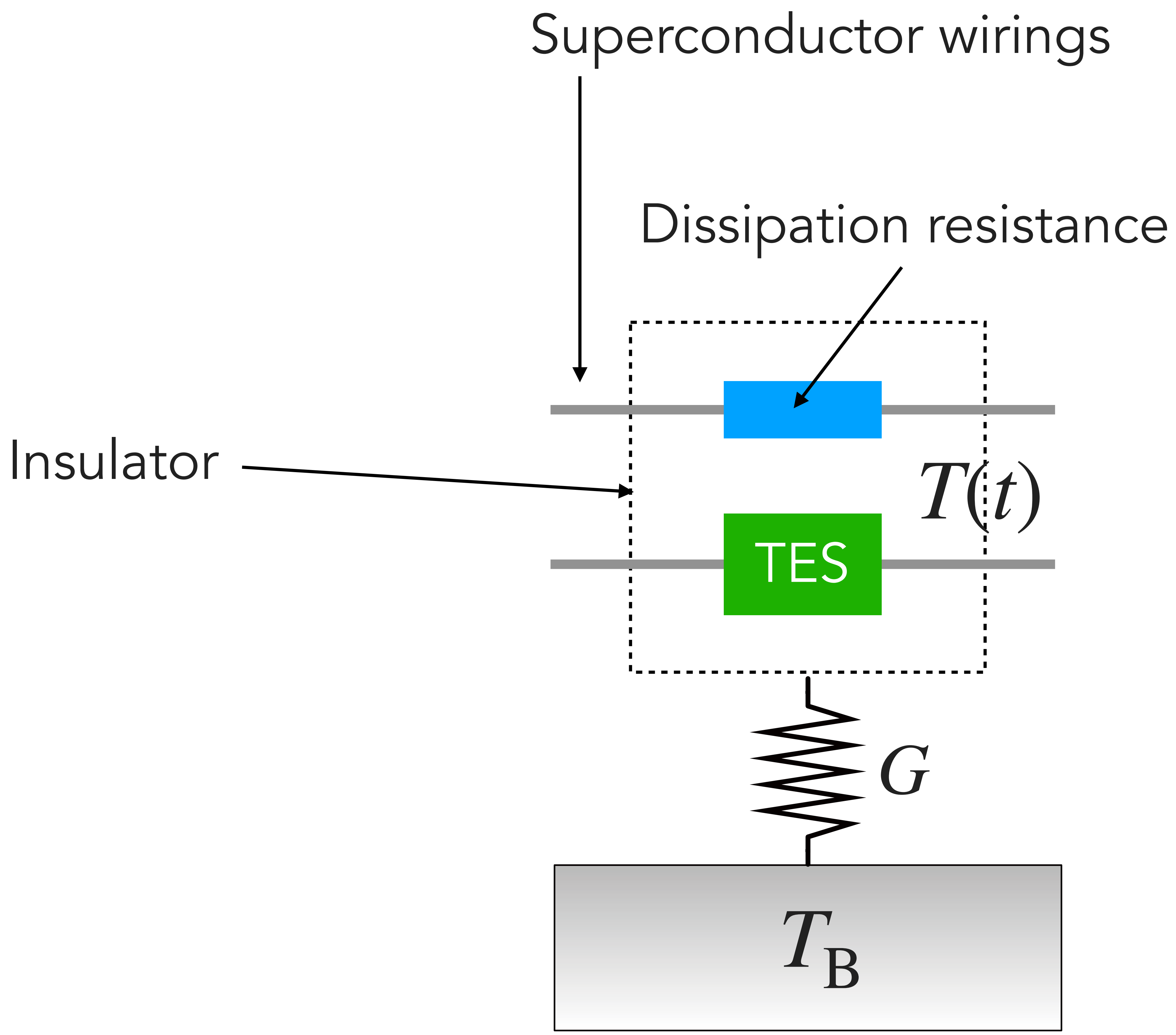

Thermalization timescales

1μs time scale is very challenging for thermal detectors.

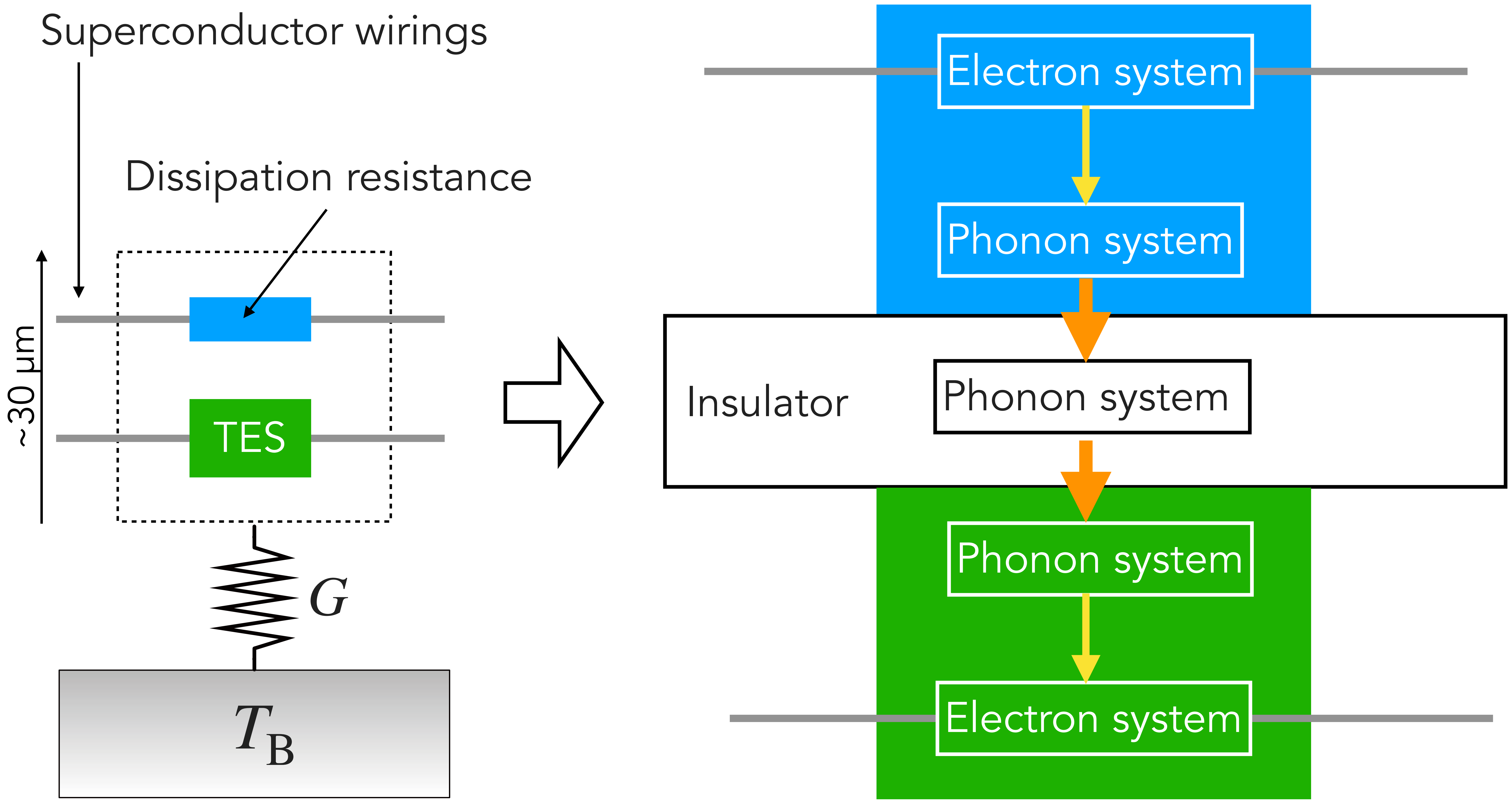

- When the device size is < ~30μm, the electron-phonon coupling will be a bottleneck of energy transfer.
- Electron-phonon coupling time scales of metals at cryogenic temperature are independent of the size and $\tau_{e-ph} \propto T^{-4}$

Wellstood, Urbina, & Clarke (1994)

To obtain $\tau_{e-ph} \ll 8\ \mu s$

$\Rightarrow T \geq 200$ mK

Note: In most X-ray μ-calorimeters, the electron system of the X-ray absorber is directly connected to the electron system of TES.

Constraint on α from NEP and saturation power

$$NEP^2 = 2k_B T^2 G = 2k_B T P_{sat} \alpha \qquad \alpha \gg 1$$

Case	0	1	2	3	4	
NEP	2.00E-17	2.00E-16	2.00E-17	6.00E-17	1.00E-16	W Hz-1/2
NEP^2	4.00E-34	4.00E-32	4.00E-34	3.60E-33	1.00E-32	W2 Hz-1
Psat	1.00E-11	1.00E-11	1.00E-12	3.33E-12	3.33E-12	W
T	0.2	0.2	0.2	0.2	0.2	K
alpha	7.24E+00	7.24E+02	7.24E+01	1.96E+02	5.43E+02	
	marginal	large margin	Good	Good	large margin	

➡ We need to relax the requirements from the present case 0 to cases 2 or 3.

Design parameters for Case 3

$$\tau_{-} = \frac{Cn}{G\alpha} = \frac{CTn}{P_{\rm sat}\alpha^2}$$

$$P_{\rm sat} = \frac{GT}{\alpha}$$

NEP	6E-17	W Hz-1/2
Psat	3.3E-12	W
tau-	8E-06	s
T	0.2	K
alpha	70	-
n	3	-
C	2.2E-13	J/K
G	1.2E-09	W/K

C → Possible with ~ 30 μm square TES + small resistor

G → Possible with a SiNx membrane.

➡ Case 3 seems feasible.

Summary

- Introduction to microcalorimeters
  - Three thermometer types are available.
- Basics of TES microcalorimeters
  - ETF and response time
  - Optimal filter (Wiener filter)
  - Energy resolution and NEP
  - Saturation
- Basics of TES bolometers
  - NEP, usable frequency range, saturation
- Example application
  - 0-th order design study of the new TES bolometers for non-astronomy application
    - Design solution seems to exist if some of the requirements are relaxed a little.

Example application

X-ray astronomy (Semiconductor-type)
Nuclear spectroscopy (MMC)

Martial science (TES μ-calorimeter)

New non-astronomy application (TES bolometer)

References

Fleischmann, Enss & Seidel (2005): Cryogenic Particle Detection, Topics Appl. Phys. 99, 151–217

Hayashi (2019): PhD thesis, University of Tokyo

Hayashi, .. KM + (2018): J. Low Temp. Phys., 193, 1282 - 1286,

Hitomi collaborations incl. KM (2016): Nature, 535, 117

Hengstler+ (2015): Phys. Scr. 2015 014054

Irwin (1995): Appl. Phys. Lett. 66, 1998–2000

Irwin & Hilton (2005): Cryogenic Particle Detection, Topics Appl. Phys. 99, 63–152

Mather (1982): Appl. Opt. 21, 1125

McCammon (2005): Cryogenic Particle Detection, Topics Appl. Phys. 99, 1–36

Mitsuda (2016): Physica C, 530, page 93 - 97

Moseley, Mather, & McCammon (1984): Journal of Applied Physics 56, 1257

Muramatsu, .. KM+ (2016): J. Low Temp. Phys., 184, 91 - 96

Muramatsu, .. KM+ (2017): IEEE Trans. on Appl. Supercond., 27, 2101204

Szymkowiak+ (1993): J. of Low Temp. Phys, 93, 281-285

Wellstood, Urbina, & Clarke (1994): Phys. Rev. B 49, 5942

Yamasaki, KM+ (2015): J. Low Temp. Phys., 181, 59 - 67

Yoshimoto, KM+ (2019): J. Low Temp. Phys., 194, 418 - 425